Diverse Supramolecular Architectures Having Well-Defined Void Spaces Formed from a Pseudorotaxane Cation: Influential Role of Metal Dithiolate Coordination Complex Anions

ARTICLE *in* CRYSTAL GROWTH & DESIGN · APRIL 2014

Impact Factor: 4.89 · DOI: 10.1021/cg500039y

1 AUTHOR:

Vedichi Madhu
Karunya University
13 PUBLICATIONS **96** CITATIONS

SEE PROFILE

CRYSTAL GROWTH & DESIGN

Article

pubs.acs.org/crystal

Diverse Supramolecular Architectures Having Well-Defined Void Spaces Formed from a Pseudorotaxane Cation: Influential Role of Metal Dithiolate Coordination Complex Anions

Vedichi Madhu[†,‡] and Samar K. Das*[,†]

[†]School of Chemistry, University of Hyderabad, Central University P.O., Gachi Bowli, Hyderabad 500046, India

[‡]Department of Chemistry, Karunya University, Coimbatore 641 114, India

Supporting Information

ABSTRACT: This paper describes the influence of a group of classical inorganic coordination complex anions on assembling a particular pseudorotaxane cation (the crown ether, dibenzo-24-crown-8 threaded by an axle, 1,2-bis(4,4′-bipyridinium) ethane) resulting in a series of supramolecular ion pair compounds, namely, [pseudorotaxane][Cu(mnt)$_2$] (**1**), [pseudorotaxane][Ni(mnt)$_2$] (**2**), [pseudorotaxane][Pd(mnt)$_2$] (**3**), and [pseudorotaxane][Zn(dmit)$_2$] (**5**) of varying dimensions in terms of their topology; dithiolene = mnt^{2-}(1,2-dicyanoethylenedithiolate) and dmit^{2-}(1,3-dithiole-2-thione-4,5-dithiolate). The shapes of supramolecular framework void spaces of diverse dimensions, that are observed in the crystal structures of compounds **1**−**3**, are influenced by the geometry of particular coordination complex anions, used in the relevant synthesis, and the concerned coordination complex gets encapsulated in the void spaces of respective supramolecular pseudorotaxane frameworks. The platinum compound [pseudorotaxane][Pt(mnt)$_2$] (**4**) is found to be an exception in forming well-defined void spaces. The crystal structure of compound [pseudorotaxane][Zn(dmit)$_2$] (**5**) reveals an interesting aggregation of supramolecular ladders, in which each compartment of the ladders accommodates the complex anion Zn(dmit)$_2$]$^{2-}$. The shape of this coordination complex anion seems to be responsible for such ladderlike arrangement in the relevant crystals. Compounds **1** through **5** have been characterized by routine analysis, such as IR, ^{1}H NMR, UV−Vis−NIR, and electron paramagnetic resonance spectroscopic techniques including elemental analysis, and unambiguously by single crystal X-ray crystallography. The stabilization of such cationic supramolecular pseudorotaxane architectures having well-defined grid-type void spaces is achieved through hydrogen bonding interactions that include C−H···S, C−H···N, and C−H···O, and $\pi-\pi$ stacking interactions. The exchange of the complex anion in one of these ion pair compounds (compound **1**) with Br$^-$ anions (in a solid-to-solid transformation through solid−liquid interface reaction) results in the formation compound [pseudorotaxane]Br$_2$ whose X-ray powder pattern is different than that of **1** indicating a new phase formation in the crystals of [pseudorotaxane]Br$_2$.

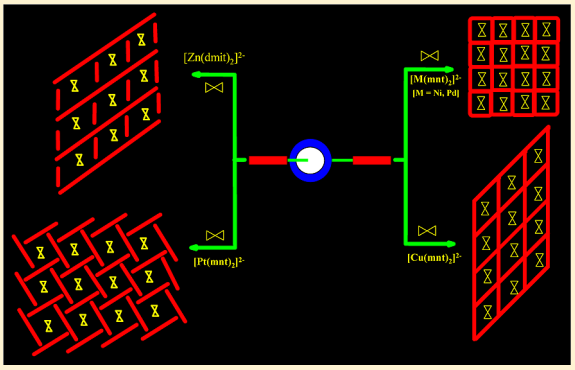

INTRODUCTION

In the mid-1980s, chemists set out to investigate the synthetic strategies of mechanically interlocked molecules, such as catenanes, pseudorotaxanes, and rotaxanes.[1] Rotaxane is a molecular architecture, formed by a dumbbell-shaped molecule (termed as an axle) threaded through a macrocycle or wheel (e.g., a crown ether), in which the axle is restrained to remain inside the wheel by suitable stopper groups. The stopper groups seem to prevent unthreading. In contrast, pseudorotaxane is formed by an axle (devoid of the stopper part) threaded into the wheel (Scheme 1). In this case, the axle is generally stabilized by noncovalent interactions such as hydrogen bonding or $\pi-\pi$ stacking interactions with the ring. These noncovalent supramolecular interactions are accountable to this threading. As per the definition of pseudorotaxane, at least one of the stoppers should be missing from the dumbbell-shaped component (axle).[2]

In rotaxane/pseudorotaxane chemistry, most of the synthetic strategies reported so far include the reorganization of building blocks by noncovalent interactions such as hydrogen bonding,[3] metal−ligand coordination,[4] $\pi-\pi$ stacking interactions,[5] donor−acceptor interactions,[6] and charge-transfer interactions.[7] Sauvage and co-workers[8] introduced a new synthetic strategy that uses a transition metal as a template to obtain interlocked molecular assemblies of rotaxanes. Loeb and co-workers have used 1,2-bis(4,4′-bipyridinium)ethane as "axle" and dibenzo[24]crown-8 ether (DB24C8) as "wheel" to construct

Received: January 8, 2014
Revised: March 17, 2014
Published: April 18, 2014

   dx.doi.org/10.1021/cg500039y | *Cryst. Growth Des.* 2014, 14, 2343−2356

Scheme 1

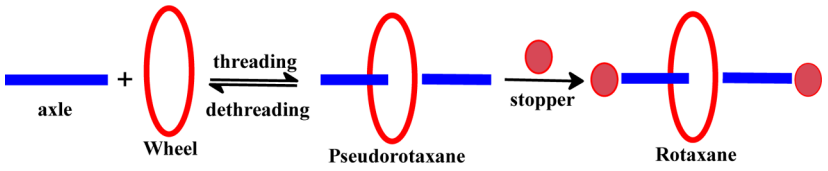

a variety of interlocked molecules and materials by means of the self-assembly strategy.[9−13] The same group used transition metal ion "nodes" to synthesize one-, two-, or three-dimensional (1D, 2D, or 3D) metal−ligand frameworks with rotaxanes as bridging ligands.[14] Supramolecular self-assembly of pseudorotaxane polymers from complementary homoditopic building blocks consisting of bis(dibenzo-24-crown-8) esters and 1,10-bis-[*p*-(benzylammoniomethyl)phenoxy] alkane bis-(hexafluorophosphate) has been reported by Gibson et al.[15] There are some reports on supramolecular polypseudorotaxanes that are shown to be formed by the combination of $\pi-\pi$ and hydrogen bonding interactions in a self-assembly process leading to a chainlike structure.[16a,b] The noncovalent interactions among pseudorotaxanes leading to supramolecular architectures are now well-established.[16c,m] However, the formation of noncovalent supramolecular architectures of diverse topology from a pseudorotaxane, driven by an inorganic coordination complex, is not much explored. We have chosen metal bis(dithiolene) coordination complexes $[M(dithiolato)_2]^{2-}$ as counteranions of a pseudorotaxane cation (Scheme 2) to generate diverse supramolecular architectures of

Scheme 2. Structural Representations of Compounds 1−5

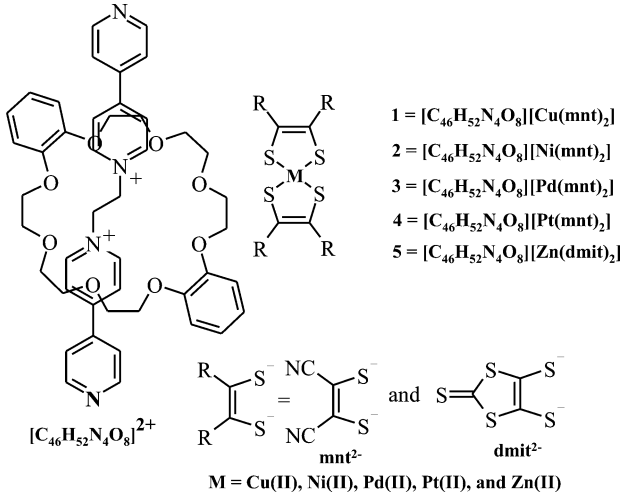

the pseudorotaxane because these dithiolene complexes in recent times have been used as an active component for the generation of useful building blocks for the design and synthesis of organic/inorganic hybrids owing to their strong intermolecular interactions through S···S contacts.[17]

We desire to describe herein the synthesis and structural characterization of a $\{[pseudorotaxane]^{2+}[M(dithiolato)_2]^{2-}\}$ system with inorganic coordination complex anions $[M(mnt)_2]^{2-}$ (M = Cu^{2+}, Ni^{2+}, Pd^{2+}, and Pt^{2+}) and $[Zn(dmit)]^{2-}$ that are supramolecularly associated with cationic pseudorotaxane resulting in the formation of diverse noncovalent pseudorotaxane architectures in compounds **1**−**5** as shown in Schemes 2 and 3. The structural analysis of compounds **1**−**5** reveals the abundance of noncovalent supramolecular grid-type channels/void spaces of diverse shapes depending on a particular coordination complex anion ($[M(mnt)_2]^{2-}$, $[Zn(dmit)_2]^{2-}$) used that is accommodated in the relevant channel/void space (Scheme 3).

EXPERIMENTAL DETAILS

Materials. The solvents used for spectral analyses were distilled according the standard procedures.[18] Disodium maleonitriledithiolate [the disodium salt of 1,2-dicyanoethylenedithiolate (Na_2mnt)] and the compounds $[Bu_4N]_2[M(mnt)_2]$ (M = Cu^{2+}, Ni^{2+}, Pd^{2+}, and Pt^{2+}) were prepared according to a synthetic procedure described in the literature.[19] Bis(tetrabutylammonium)bis(1,3-dithiole-2-thione-4,5-dimercapto)zincate, $[Bu_4N]_2[Zn(dmit)_2]$ was prepared according to the literature method.[20] The dipyridinium axle 1,2-bis(4,4′-bipyridinium) ethane was synthesized as a PF_6 salt by a known procedure.[9,10]

Physical Measurements. Microanalytical (C, H, N, S) data were obtained with a FLASH EA 1112 Series CHNS analyzer. Infrared (IR) spectra were recorded on KBr pellets with a JASCO FT/IR-5300 spectrometer in the region of 400−4000 cm^{-1}. Electronic spectra were obtained on a UV-3101PC/UV−VIS−NIR spectrophotometer (Shimadzu), equipped with a diffuse reflectance accessory (reflectance spectra were recorded on KBr pellets). The diffuse reflectance spectra, obtained, were then Kubelka−Munk corrected. The electron spin resonance (ESR) spectra were recorded on a (JEOL) JESFA200 ESR spectrometer. Powder X-ray diffraction data were collected on a Phillips PW 3710 diffractometer. ^1H NMR spectra were recorded on Bruker DRX-400 spectrometer using $Si(CH_3)_4$ (TMS) as an internal standard in DMSO-d_6 solvent.

Synthesis and Characterization. *Synthesis of [Pseudorotaxane][Cu(mnt)$_2$] (**1**).* [1,2-Bis(4,4′-bipyridinium)ethane]-$(PF_6)_2$ (50 mg, 0.080 mmol) was suspended in a 15 mL of dry CH_3CN. To this solution was added dibenzo-24-crown-8 (40 mg, 0.089 mmol). It was then stirred for 30 min at room temperature under dry N_2 atmosphere giving rise to yellow solution; to this reaction mixture was added $[Bu_4N]_2[Cu(mnt)_2]$ (60 mg, 0.072 mmol) in 15 mL of dry CH_3CN. It was further stirred for 5−10 min at room temperature, and the formation of resulting precipitate was removed by filtration. The filtrate (red-brown in color) was allowed to stand for one week in an open beaker, whereby cubic dark brown colored crystals appeared. The crystals of compound **1** were collected by decantation of solvent, washed with ether, and dried in air at room temperature. The crystals were suitable for single crystal X-ray crystallography. Yield: 40 mg (49% based on copper). Anal. Calcd for $C_{54}H_{52}N_8O_8S_4Cu$ (1132.82 g mol^{-1}): C, 57.25; H, 4.63; N, 9.89; S, 11.32. Found: C, 58.08; H, 5.13; N, 10.03; S, 11.54. IR (KBr pellet) (ν/cm^{-1}): 3061(m, Ar-H), 2895(w), 2189(s, C≡N), 1642(s, pyridine), 1545(s, pyridinium), 1524(w), 1503(w), 1456(w, C═C, mnt), 1406(w, C-S), 1350(w), 1252(w), 1213(w), 1146(s, C-O-C), 1100(w), 1051(w), 939(w, C═C, aromatic), 814 (m), 745(w), 718(w), 509(w).

*Synthesis of [Pseudorotaxane][Ni(mnt)$_2$] (**2**).* Pseudorotaxane was prepared by the same synthetic procedure, as described in the preparation of **1**, from [1,2-bis(4,4′-bipyridinium)ethane]$(PF_6)_2$ (50 mg, 0.08 mmol) and dibenzo-24-crown-8 (42 mg, 0.093 mmol) in CH_3CN (15 mL). To the yellowish solution of pseudorotaxane was added $[Bu_4N]_2[Ni(mnt)_2]$ (58 mg, 0.070 mmol) in CH_3CN (15 mL), and then it was continuously stirred for 5 min at room temperature. The formation of small amount of precipitate was filtered off. The filtrate (red-brown in color) was allowed to stand for one week in an

dx.doi.org/10.1021/cg500039y | *Cryst. Growth Des.* 2014, 14, 2343−2356

Scheme 3. Representation of Various Noncovalent Supramolecular Pseudorotaxane Architectures (Solid Red Color) Having Grid-type Channels That Accommodate the Coordination Complex Anions $[M(mnt)_2]^{2-}$ (M = Cu, Ni, Pd, and Pt) and $[Zn(dmit)_2]^{2-}$

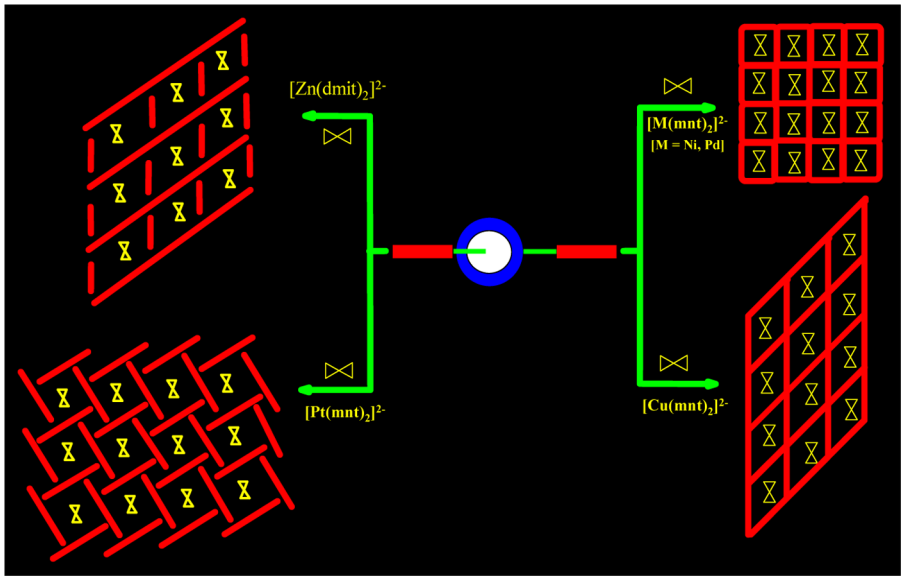

open beaker at room temperature. Red needle-shaped crystals, obtained, were collected by decantation of solvent, washed with ether, and dried in air. The crystals were suitable for single crystal X-ray crystallography. Yield: 34 mg (43% based on nickel). Anal. Calcd for $C_{54}H_{52}N_8O_8S_4Ni$ (1127.99 gmol^{-1}): C, 57.50; H, 4.65; N, 9.93; S, 11.37. Found: C, 56.98; H, 4.92; N, 9.54; S, 10.95. IR (KBr pellet) (ν/cm^{-1}): 3526(m), 3050(m, Ar-H), 2359(w), 2195(s, C≡N), 1635(s, pyridine), 1543(s, pyridinium), 1483(w, C═C, mnt), 1410(w, C-S), 1195(s), 1149(s, C-O-C), 862(w, C═C, aromatic), 814(m), 719(w). ^{1}H NMR (DMSO-d_6): δ (ppm) 9.17(d, 4H, J = 6.8 Hz, *ortho*-N$^+$), 8.91(d, 4H, J = 4.8 Hz, *ortho*-N), 8.73(d, 4H, J = 5.8 Hz, *meta*-N$^+$), 8.08(d, 4H, J = 4.8 Hz, *meta*-N), 6.92(m, 4H, *ortho*-O), 6.85(m, 4H, *meta*-O), 5.27(s, 4H, CH$_2$−N$^+$), 3.5(s, 24H, CH$_2$-crown).

*Synthesis of [Pseudorotaxane][Pd(mnt)$_2$] (**3**).* Pseudorotaxane was prepared by the same synthetic procedure, as given in the synthesis of **1**, from [1,2-bis(4,4′-bipyridinium)ethane](PF$_6$)$_2$ (52 mg, 0.082 mmol) and dibenzo-24-crown-8 (39 mg, 0.087 mmol) in CH$_3$CN (15 mL). To the yellow solution of pseudorotaxane was added [Bu$_4$N]$_2$[Pd(mnt)$_2$] (65 mg, 0.074 mmol) in CH$_3$CN (15 mL), and then the mixture was stirred for 5 min at room temperature. The resulting precipitate (appeared as small amount) was filtered off; the filtrate (green colored) was allowed to stand for a week in an open beaker. Greenish-black crystals were collected by decantation of solvent, washed with ether, and dried in air at room temperature. Yield: 38 mg (51% based on Pd). Anal. Calcd for $C_{54}H_{52}N_8O_8S_4Pd$ (1175.68 g mol^{-1}): C, 55.16; H, 4.46; N, 9.53; S, 10.91. Found: C, 54.87; H, 4.75; N, 9.89; S, 11.12. IR (KBr pellet) (ν/cm^{-1}): 3051(m, Ar-H), 2870(w), 2191(s, C≡N), 1643(s, pyridine), 1593(s, pyridinium), 1504(w), 1485(w, C═C, mnt), 1404(w, C-S), 1352(w), 1249(w), 945(w, C═C, aromatic), 862(m), 814(w), 738(w), 719(w), 507(w). ^{1}H NMR (DMSO−d_6): δ (ppm) 9.21-(broad, 4H, *ortho*-N$^+$), 8.96(broad, 4H, *ortho*-N), 8.78(broad, 4H, *meta*-N$^+$), 8.11(broad, 4H, *meta*-N), 6.93(m, 4H, *ortho*-O), 6.89(m, 4H, *meta*-O), 5.31(s, 4H, CH$_2$−N$^+$), 3.67(s, 24H, CH$_2$-crown).

*Synthesis of [Pseudorotaxane][Pt(mnt)$_2$] (**4**).* To the yellowish solution, obtained from [1,2-bis(4,4′-bipyridinium)ethane](PF$_6$)$_2$ (50 mg, 0.080 mmol) and dibenzo-24-crown-8 (40 mg, 0.090 mmol) in CH$_3$CN (15 mL), was added [Bu$_4$N]$_2$[Pt(mnt)$_2$] (70 mg, 0.070 mmol) in CH$_3$CN (15 mL), and the mixture was stirred for 5 min at room temperature. A small amount of precipitate was found to be formed, which was removed by filtration. The filtrate (red colored) was allowed to stand at room temperature, and after one week black-colored crystals of **4** were collected by decantation of solvent, washed with ether, and dried in air. Yield: 35 mg (40% based on Pt). Anal. Calcd for $C_{54}H_{52}N_8O_8S_4Pt$ (1264.37 g mol^{-1}): C, 51.29; H, 4.14; N, 8.86; S, 10.14. Found: C, 51.67; H, 3.89; N, 8.24; S, 10.36. IR (KBr pellet) (ν/cm^{-1}): 3050(m, Ar-H), 2359(w), 2194(s, C≡N), 1637(s, pyridine), 1541(s, pyridinium), 1456(w, C═C, mnt), 1421(w, C-S), 1195(w), 1149(s, C-O-C), 862(w), 814(m), 719(w), 567(w), 505(w). ^{1}H NMR (DMSO-d_6): δ (ppm) 9.22(broad, 4H, *ortho*-N$^+$), 8.95-(broad, 4H, *ortho*-N), 8.77(broad, 4H, *meta*-N$^+$), 8.10(broad, 4H, *meta*-N), 6.89(m, 4H, *ortho*-O), 6.82(m, 4H, *meta*-O), 5.31(s, 4H, CH$_2$−N$^+$), 3.44(s, 24H, CH$_2$-crown).

*Synthesis of [Pseudorotaxane][Zn(dmit)$_2$] (**5**).* To the yellowish solution of pseudorotaxane (prepared by the procedure as given in the synthesis of **1**) was added [Bu$_4$N]$_2$[Zn(dmit)$_2$] (70 mg, 0.074 mmol) in CH$_3$CN (15 mL), and the mixture was stirred for 5 min at room temperature. The resulting slight quantity of precipitate was filtered off. The filtrate (red colored) was allowed to stand for one week in an open beaker at room temperature. The red-colored crystals of **5** obtained during this time were collected, washed with ether, and dried in room temperature. Yield: 44 mg (50% based on Zn). Anal. Calcd for $C_{52}H_{52}N_4O_8S_{10}Zn$ (1246.95 g mol^{-1}): C, 50.08; H, 4.20; N, 4.49; S, 25.71. Found: C, 50.23; H, 4.53; N, 4.77; S, 24.83. IR (KBr pellet) (ν/cm^{-1}): 3435(w), 2920(m, Ar-H), 1637(s, pyridine), 1538(s, pyridinium),1509(w), 1412(w, C═C, dmit), 1113(s, C-O-C), 1056(m, C═S), 1022(m, C═S), 815(m), 740(w), 715(w), 569(w), 509(w). ^{1}H NMR (DMSO-d_6): δ (ppm) 9.11(d, 4H, J = 6.8 Hz, *ortho*-N$^+$), 8.89(broad, 4H, *ortho*-N), 8.72(d, 4H, J = 5.8 Hz, *meta*-N$^+$), 8.03(broad, 4H, *meta*-N), 6.92(m, 4H, *ortho*-O), 6.87(m, 4H, *meta*-O), 5.25(s, 4H, CH$_2$−N$^+$), 3.34(s, 24H, CH$_2$-crown).

X-ray Analyses. *Single Crystal Structure Determination.* Single crystal data were measured at room temperature for compounds **1**−**5** on a Bruker SMART APEX CCD, area detector system [λ(Mo Kα) = 0.7103 Å], graphite monochromator, 2400 frames recorded with an ω scan width of 0.3°, each for 8 s, crystal−detector distance 60 mm, collimator 0.5 mm. Data reduction was by SAINTPLUS,[21] an empirical absorption correction was performed using method SADABS,[22] and the structure solution was performed using SHELXS-97[23] and refined using SHELXL-97.[24] Hydrogen atoms on the pseudorotaxanes were introduced on calculated positions and included in the refinement riding on their respective parent atoms. Hydrogen bonding interactions were discussed based on respective D−H···A contacts. A summary of the crystallographic data and structural determination for compounds **1**−**5** is provided in Tables 1 and 2.

dx.doi.org/10.1021/cg500039y | *Cryst. Growth Des.* 2014, 14, 2343−2356

Table 1. Crystal Data and Structural Refinement for Compounds 1 and 2

	1	2
empirical formula	$C_{54}H_{52}CuN_8O_8S_4$	$C_{108}H_{104}Ni_2N_{16}O_{16}S_8$
formula weight	1132.87	2255.97
T [K]	298(2)	298(2)
λ [Å]	0.71073	0 71073
crystal system	monoclinic	triclinic
space group	$C2/c$	$P\bar{1}$
a [Å]	14.630(3)	12.2467(14)
b [Å]	20.316(4)	12.6654(14)
c [Å]	19.240(4)	20.006(2)
α [deg]		100.451(2)
β [deg]	110.17(3)	98.868(2)
γ [deg]		114.245(2)
V [Å^3]	5367.9(19)	2690.5(5)
Z	4	1
D_{calc} [Mg m^{-3}]	1.402	1.392
μ [mm^{-1}]	0.624	0.577
F[000]	2356	1176
crystal size [mm^3]	0.22 × 0.16 × 0.11	0.21 × 0.16 × 0.070
θ range for data collection [deg]	1.79−25.00	1.07−26.37
reflections collected/unique	25544/4731	29020/10930
R (int)	0.0790	0.0774
refinement method	full-matrix least-squares on F^2	
data/restraints/parameters	4731/0/339	10930/0/676
goodness-of-fit on F^2	0.880	0.849
R_1/wR_2 [$I > 2\sigma(I)$]	0.0523/0.1177	0.0637/0.1132
R_1/wR_2 (all data)	0.1154/0.1347	0.1995/0.1500
largest diff peak/hole [e Å^{-3}]	0.704/−0.178	0.326/−0.205

RESULTS AND DISCUSSION

Synthesis. The formation of [pseudorotaxane]$(PF_6)_2$ from the PF_6 salt of 1,2-bis(4,4′-bipyridinium) ethane and the crown ether (DB24C8) in acetonitrile solvent is shown in Scheme 4. The ion-pair type of compounds **1**−**5** were synthesized by the combination of 1 equiv of [pseudorotaxane]$(PF_6)_2$ and 1 equiv of $[Bu_4N]_2[M(dithiolene)_2]$ (M = Cu(II) (**1**), Ni(II) (**2**), Pd(II) (**3**), Pt(II) (**4**), and Zn(II) (**5**); dithiolene = mnt^{2-} and $dmit^{2-}$) in acetonitrile at room temperature that result in the formation of [pseudorotaxane][M(dithiolene)$_2$] ion-pair aggregations as presented in Scheme 5.

Each of these resulting compounds **1**−**5** consists of $[pseudorotaxane]^{2+}$ as a cation and $[M(dithiolene)_2]^{2-}$ as an anion in 1:1 ratio. The title compounds are not freely soluble in common organic solvents; thus the NMR studies were performed in DMSO. Since DMSO is a polar solvent, it would destroy any noncovalent interactions resulting in free pyridinium axle, free crown ether and anion (which contains no protons). Thus all solution spectra are almost identical.

X-ray Crystallographic Studies. *Crystal Structure Description of [Pseudorotoxane][Cu(mnt)$_2$] (1).* Crystals of compound [pseudorotoxane][Cu(mnt)$_2$] (**1**), suitable for single-crystal X-ray diffraction studies, were grown from acetonitrile solvent. Compound **1** crystallizes in monoclinic system with space group $C2/c$ and single-crystal X-ray data, obtained at 298 K, are summarized in Table 1. A thermal ellipsoidal plot of the compound **1** is depicted in Figure S1 (see Supporting Information section). The molecular structure of **1** shows the abundance of $[pseudorotaxane]^{2+}$ as a dication and $[Cu(mnt)_2]^{2-}$ as an dianion in 1:1 ratio in the solid state (Figure 1). The selected bond lengths and bond angles of compound **1** are presented in Table S1. The cationic part $[pseudorotaxane]^{2+}$ is formed by the 1,2-bis(4,4′-bipyridinium)-ethane axle, threaded through a DB24C8 wheel (crown ether) and stabilized by the combination of hydrogen bonding and $\pi-\pi$ interactions (vide infra). The $[Cu(mnt)_2]^{2-}$ complex anion, in compound **1**, possess the Cu(II) ion in a distorted square planar environment (see Figure S2 in Supporting Information). The anion exhibits nonplanar geometry, in which each Cu atom is surrounded by four sulfur atoms from two mnt^{2-} ligands. The distortion of the chelate rings (from two mnt^{2-} ligands) can be measured by their dihedral angle (35.58°). Copper ion is deviated from the least-squares plane by 0.0618 Å; a similar deviation has been reported earlier for a nonplanar $[Cu(mnt)_2]^{2-}$.[25]

The C−H···S and C−H···N hydrogen bonds [hydrogen atoms are from the axle, 1,2-bis(4,4′−bipyridinium) ethane], that involve both $[Cu(mnt)_2]^{2-}$ complex anion and $[pseudorotaxane]^{2+}$ dication, play a significant role in constructing the three-dimensional supramolecular architecture in the crystal structure of compound [pseudorotaxane][Cu(mnt)$_2$] (**1**). We have found that, the C−H···S hydrogen bonds are formed by the interactions of $[pseudorotaxane]^{2+}$ hydrogen atoms and the dithiolato sulfur atoms of $[Cu(mnt)_2]^{2-}$ as revealed in Figure 2. Figure 2a shows that, each $[pseudorotaxane]^{2+}$ cation interacts with four different $[Cu(mnt)_2]^{2-}$ anions through the combination of both C−H···S and C−H···N intermolecular hydrogen bonding interactions. Likewise, each $[Cu(mnt)_2]^{2-}$ complex anion interacts with four different pseudorotaxane dications through the assistance of C−H···S and C−H···N intermolecular hydrogen bonding interactions as shown in Figure 2b. It is remarkable that all the "S" and "N" atoms of the complex anion are exclusively involved in hydrogen bonding interactions. Figure 2b clearly reveals that the assembly of cationic pseudorotaxanes form the framework around $[Cu(mnt)_2]^{2-}$ complex anion. The C···S and H···S separations fall in range of 3.483(4)−3.712(5) Å and 2.71−2.84 Å respectively, and the relevant C−H···S bond angles in the crystal structure of compound **1** fall in the range from 140.6° to 157.6°. These parameters are consistent with those of other related systems reported earlier.[26] The relevant C−H···N hydrogen bonding parameters, associated with the interactions between $[pseudorotaxane]^{2+}$ cation and $[Cu(mnt)_2]^{2-}$ anion, vary from 3.489(6) to 3.669(7) Å and 2.59 to 2.82 Å respectively. These data also fall in the range for C−H···N hydrogen bonding parameters of the relevant reported systems.[27] The hydrogen bond distances in the crystal structure of compound **1** are described in Table 3. The involvement of $[Cu(mnt)_2]^{2-}$ anion in hydrogen bonding interactions with its surroundings in the crystal structure of compound **1** is shown in Figure S3 (Supporting Information). As the electronegativity difference between H and S (δ = 0.38, Pauling scale) is very small compared to those between H and X (X = Cl, N, O), the hydrogen bonds involving H and S will necessarily be weak due to the poorer match between the hard proton and soft sulfur.[28] Even though, with the aid of supramolecular interactions with metal coordination complex anion $[M(dithiolato)_2]^{2-}$, the pseudorotaxane cation forms network type noncovalent architectures having void spaces, in which the complex anions are located, the present system can not be described as a host−guest system because it is a kind of salt of pseudorotaxane cation and coordination complex anion, stabilized by complementary effect. In the supramolecular

dx.doi.org/10.1021/cg500039y | Cryst. Growth Des. 2014, 14, 2343−2356

Table 2. Crystal Data and Structural Refinement for Compounds 3, 4, and 5

	3	4	5
empirical formula	$C_{108}H_{104}N_{16}O_{16}Pd_2S_8$	$C_{54}H_{52}PtN_8O_8S_4$	$C_{104}H_{104}N_8O_{16}S_{20}Zn_2$
formula weight	2351.35	1264.37	2493.89
T [K]	298(2)	298(2)	298(2)
λ [Å]	0.71073	0.71073	0.71073 A
crystal system	triclinic	monoclinic	triclinic
space group	$P\bar{1}$	$P2_1/c$	$P\bar{1}$
a [Å]	12.2674(9)	6.9946(5)	12.2553(7)
b [Å]	12.6097(9)	26.3116(19)	13.9830(8)
c [Å]	20.1508(14)	14.0147(10)	19.4427(11)
α [deg]	100.1080(10)		96.9870(10)
β [deg]	99.2670(10)	97.4550(10)	91.8630(10)
γ [deg]	114.1570(10)		114.7970(10)
V [Å^3]	2704.3(3)	2557.5(3)	2989.2(3)
Z	1	2	1
D_{calc} [Mg m^{-3}]	1.444	1.642	1.385
μ [mm^{-1}]	0.559	2.972	0.813
F[000]	1212	1276	1292
crystal size [mm^3]	0.1 × 0.1 × 0.28	0.16 × 0.36 × 0.12	0.3 × 0.20 × 0.14
θ range for data collection [deg]	1.84−24.71	1.55−26.03	1.06−24.71
reflections collected/unique	25649/9202	26319/5051	22335/8540
R(int)	0.0588	0.0584	0.0816
refinement method		full-matrix least-squares on F^2	
data/restraints/parameters	9202/0/676	5051/0/340	8540/0/676
goodness-of-fit on F^2	0.825	1.135	0.880
R_1/wR_2 [$I > 2\sigma(I)$]	0.0521/0.0979	0.0276/0.0683	0.0689/0.1773
R_1/wR_2 (all data)	0.1265/0.1180	0.0304/0.0696	0.1469/0.2064
largest diff peak/hole [e Å^{-3}]	0.521/−0.242	1.255/−0.765	0.720/−0.278

Scheme 4. Schematic Presentation Showing the Formation of [Pseudorotaxane]$(PF_6)_2$

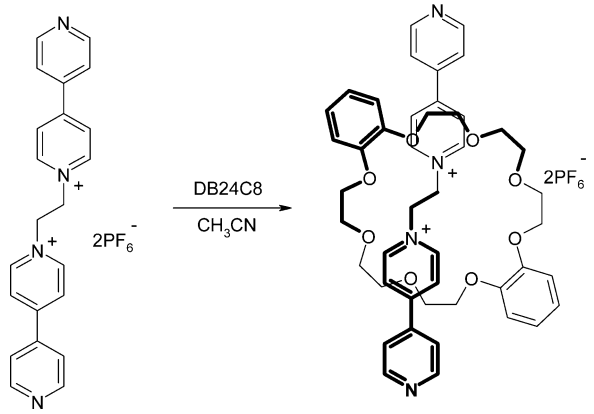

architecture, each void space accommodates two $[Cu(mnt)_2]^{2-}$ complex anions and their surrounding environment is the part of network/architecture, constructed by eight pseudorotaxane cations. This situation is shown in Figure 3. The formation of this supramolecular construction (Figure 3) also requires $\pi-\pi$ stacking interactions (in addition to C−H···S and C−H···N hydrogen bonds, as described above). There are four kinds of $\pi-\pi$ interactions throughout the architecture in the crystal structure of compound **1**: (i) types 1 and 2, intrapseudorotaxanes $\pi-\pi$ interactions that involve the aromatic ring of the crown ether (wheel) and close by aromatic ring (to ethylenic bond) of the axle; (ii) types 3 and 4, interpseudorotaxanes $\pi-\pi$ interactions that include both aromatic rings of the axle. Types 1−4 $\pi-\pi$ interactions are presented in Figure S4 (Supporting Information). The relevant centroid-to-centroid (C_t-C_t) distances span from 3.679(7) Å to 3.751 (7) Å and the range of mean plane separations (MPS) is 3.326 Å−3.425 Å; the details are described in the caption of Figure S4 (Supporting Information). Loeb and co-workers have reported same pseudorotaxane cation using other anions, in which pseudorotaxanes associate in the solid state to form pseudopolyrotaxanes by hydrogen bonding or π-stacking.[29] Thus it is logical to say that in the present study (in the case of compound **1**), an inorganic coordination complex anion $[Cu(mnt)_2]^{2-}$ is responsible for the construction of such pseudopolyrotaxane based cationic architectures having well-defined void space, in which the complex anion is located by using its "S" and "N" atoms as H-bond acceptors as shown in Figure 3. The resulting grid type of network of pseudorotaxane cation with coordination complex anion situated in the void spaces is shown in Figure S5 (Supporting Information).

*Structural Descriptions of Compounds [Pseudorotaxane]-[Ni(mnt)$_2$] (**2**) and [Pseudorotaxane][Pd(mnt)$_2$] (**3**).* The compounds [pseudorotaxane][Ni(mnt)$_2$] (**2**) and [pseudorotaxane][Pd(mnt)$_2$] (**3**) are isostructural and crystallize in the triclinic system with space group $P\bar{1}$. The asymmetric unit of the single crystal structures of [pseudorotaxane][Ni(mnt)$_2$] (**2**) or [pseudorotaxane][Pd(mnt)$_2$] (**3**) consists of two half DB24C8 (crown ether) units, two half 1,2-bis(4,4′-bipyridinium)-ethane units, and one full $[M(mnt)_2]^{2-}$ (M = Ni and Pd) anion as shown in Figure 4. Accordingly, one formula unit of **2** and/or **3** contains one $[pseudorotaxane]^{2+}$ cation and one $[M(mnt)_2]^{2-}$ (M = Ni and Pd) anion as revealed in Figure S6 (Supporting Information). In the crystal structures of compounds **2** and **3**, the inorganic complex anion $[M(mnt)_2]^{2-}$ (M = Ni (**2**) and Pd (**3**)) exists in a planar geometry (Figure S7, Supporting Information). The nickel and palladium ions are

dx.doi.org/10.1021/cg500039y | Cryst. Growth Des. 2014, 14, 2343−2356

Scheme 5. General Synthetic Scheme for the Syntheses of [Pseudorotaxane][M(dithiolene)$_2$] in Compounds 1−5

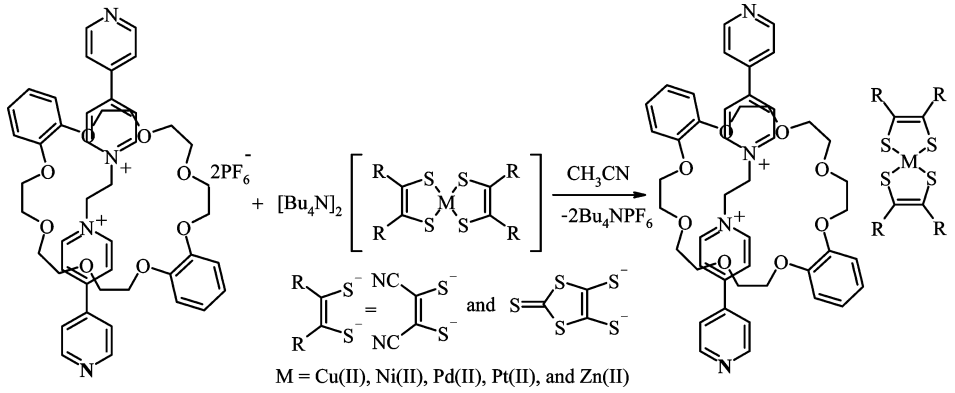

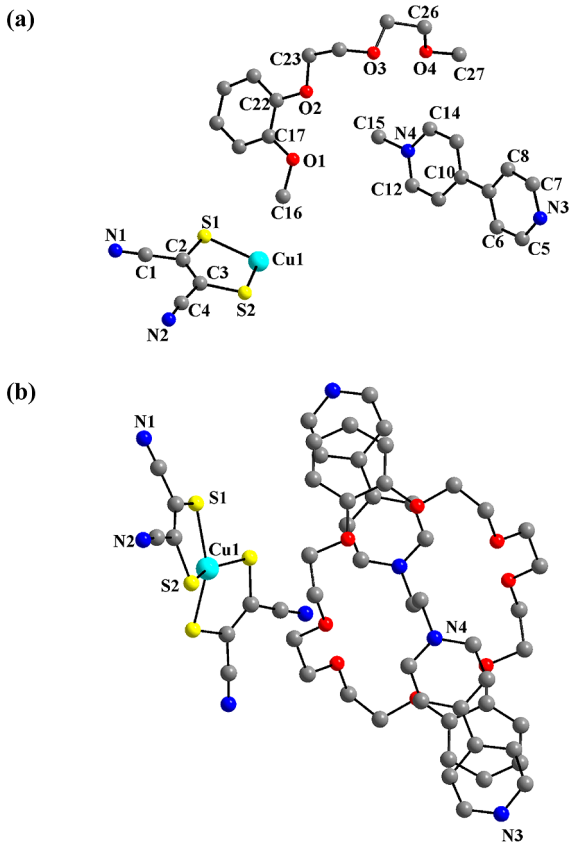

Figure 1. (a) The asymmetric unit in the crystal structure of compound **1**. (b) The molecular structure of **1** with atom labels, hydrogen atoms are omitted for clarity. Color code: N, blue; O, red; C, gray; S, yellow; Cu, cyan.

displaced by 0.029 and 0.027 Å from the respective least-squares plane in the crystal structures of compounds **2** and **3** respectively. The average Ni−S distance is 2.1634 Å in compound **2**, and the average Pd−S distance is 2.2839 Å in compound **3**. The selected bond distances and angles for compounds **2** and **3** are described in Tables S2 and S3 (Supporting Information) respectively. In the case of compound **2**, the existence intermolecular hydrogen bonding interactions between pseudorotaxane cation and $[Ni(mnt)_2]^{2-}$ anion is shown in Figure 5a, which reveals that each of $[pseudorotaxane]^{2+}$ cations interacts with two different complex anions through bifurcated C−H···S hydrogen bonds. We have also observed $\pi-\pi$ interactions in the crystal structures of compounds **2** and **3**. The combination of both intermolecular hydrogen bonding and $\pi-\pi$ interactions leads to aggregation of $[pseudorotaxane]^{2+}$ cations around the complex anion, as if the complex anion $[M(mnt)_2]^{2-}$ gets encapsulated in the void space (Figure 5b, for compound **2**). The supramolecular hydrogen bonding interactions between anion and cation for compound **3** are shown in Figure S8 (Supporting Information). The overall packing diagram in the crystal structure of compound **2** shows extended supramolecular architecture having distinct void spaces, in which the complex anions are located as shown in Figure S9 (Supporting Information). Similar supramolecular void spaces have also been observed in the crystal structure of compound **3**.

Unlike the situation in the crystal of compound [pseudorotoxane][Cu(mnt)$_2$] (**1**), in the crystal structure of compound **2** (or **3**), all the four nitrogen atoms (N1, N2, N3, and N4) of the $[Ni(mnt)_2]^{2-}$ anion are involved in forming hydrogen bonds with $[pseudorotaxane]^{2+}$ cation through C−H···N hydrogen bonding interactions. The related range of C···N and H···N intermolecular interaction distances is from 3.44(11) to 3.68(7) Å and from 2.56 to 2.75 Å respectively with relevant hydrogen bond angles in the range of 152−175.7°. The intra-pseudorotaxane C−H···O hydrogen bonding distances fall in the range of 2.4−2.96 Å with the corresponding bond angles in the range of 119.1−172.3° (compound **2**, Table 4). In the crystal of compound **3**, a similar C−H···O, C−H···N, and C−H···S hydrogen bonding pattern is observed (Table 5) as is found in the structure of compound **2**. From the $\pi-\pi$ stacking interactions, observed in the crystal structure of compounds **2** and **3**, the Ct−Ct distances are 3.663(3)−3.840(3) Å and 3.673(3)−3.834(3) Å for compounds **2** and **3** respectively. The corresponding mean plane separations (MPS) are 3.339 Å−3.840 Å (compound **2**) and 3.344−3.363 Å (compound **3**).

*Crystal Structure Description of Compound [Pseudorotaxane][Pt(mnt)$_2$] (**4**).* Compound **4**, obtained in a previously mentioned similar synthesis, crystallizes in the monoclinic system with space group $P2(1)/c$. A thermal ellipsoid plot of the compound [pseudorotoxane][Pt(mnt)$_2$] (**4**) is presented in Figure 6. The asymmetric unit in the single crystal structure of compound [pseudorotaxane][Pt(mnt)$_2$] (**4**) consists of an half pseudorotoxane unit and an half of $[Pt(mnt)_2]^{2-}$ anion as shown in Figure 6a. Thus, one formula unit of **4** contains one $[pseudorotaxane]^{2+}$ cation and one $[Pt(mnt)_2]^{2-}$ anion (Figure 6b). Selected bond distances and angles in the crystal structure of compound **4** are tabulated in Table S4 (Supporting Information). Interestingly, the [pseudorotaxane]$^{2+}$ cation interacts with two different $[Pt(mnt)_2]^{2-}$

dx.doi.org/10.1021/cg500039y | *Cryst. Growth Des.* 2014, 14, 2343−2356

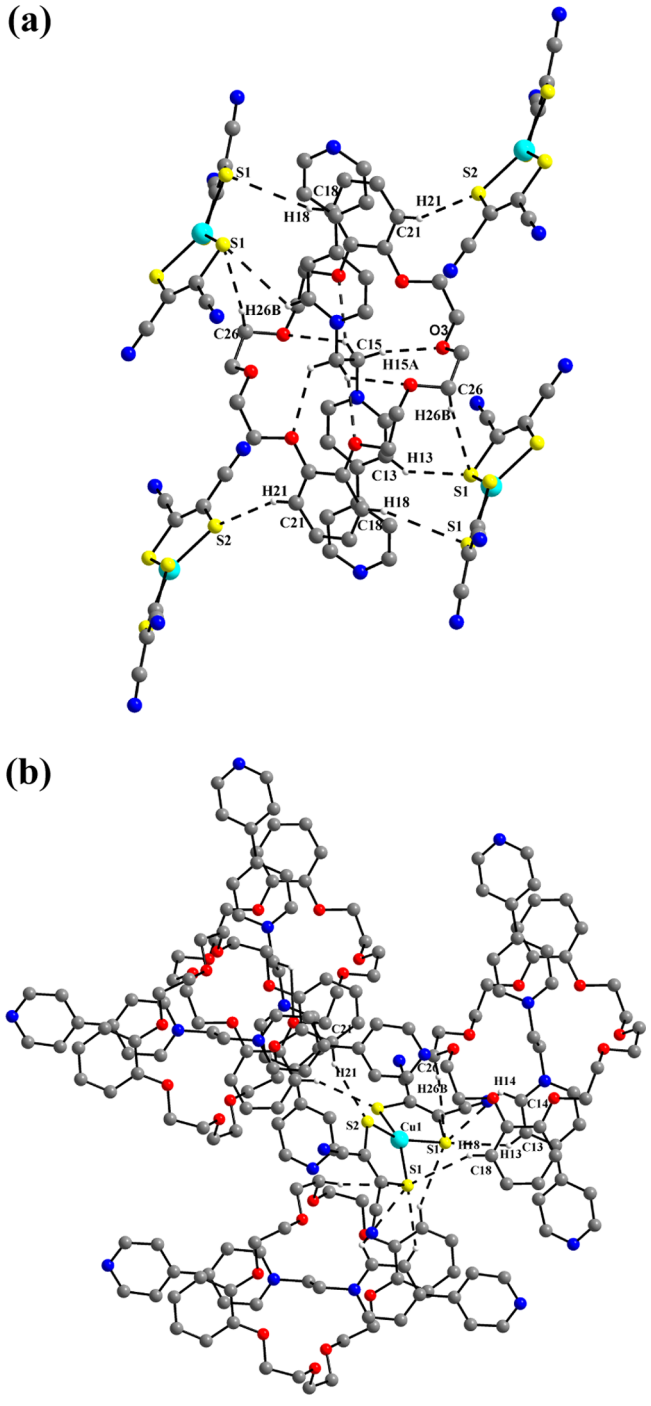

Figure 2. The C−H···S hydrogen bonding interactions in **1**: (a) the hydrogen bonding interaction between one $[pseudorotaxane]^{2+}$ cation and four $[Cu(mnt)_2]^{2-}$ anions and (b) hydrogen bonding interactions between a $[Cu(mnt)_2]^{2-}$ anion and four $[pseudorotaxane]^{2+}$ cations. Color code: N, blue; O, red; C, gray; S, yellow; Cu, cyan.

anions through four bifurcated C−H···S hydrogen bonds. Similarly, the $[Pt(mnt)_2]^{2-}$ anion is hydrogen bonded to two different cations through four bifurcated hydrogen bonds (Figure 7a). The ranges of C−H···S and C−H···O hydrogen bonding distances are 2.81−2.84 Å and 2.30−2.60 Å respectively; the corresponding C−H···S and C−H···O bond angles fall in the range of 135−173°. The relevant hydrogen bonding parameters are summarized in Table 6. The sulfur atoms of $[Pt(mnt)_2]^{2-}$ anion interact with adjacent dipyridinium axles of $[pseudorotaxane]^{2+}$ cations resulting in the formation of a chain-like arrangement (formed by C−H···S hydrogen bonds) consisting of cations and anions alternatively, as shown in Figure 7b. It is noteworthy that there are no well-defined grid-type void spaces (as found in the case of compounds **1**−**3**) in the crystal structure of compound **4**, despite the existence of hydrogen bonding and $\pi-\pi$ stacking interactions. The relevant crystal packing diagram is shown in Figure S10 (Supporting Information), which shows a situation as if the grid-type void spaces, found in the crystal structures of compounds **1**−**3**, are collapsed. The probable reason for this is the absence of intermolecular $\pi-\pi$ interactions among the axles of the pseudorotaxanes (in the crystal structure of compound **4**) that are main forces in construction of such grid type network in the crystal structures of compounds **1**−**3**. The relatively larger size of the coordination complex $[Pt(mnt)_2]^{2-}$ anion (compared to those of $[Cu(mnt)_2]^{2-}$, $[Ni(mnt)_2]^{2-}$, and $[Pd(mnt)_2]^{2-}$ complex anions in compounds **1**, **2**, and **3** respectively) probably plays an important role in making this difference.

Table 3. Hydrogen Bonds, Observed in the Crystal Structure of Compound 1[a]

D−H···A	d(D···H)	d(H···A)	d(D···A)	∠(DHA)
C21−H21···S2 #3	0.93	2.84	3.712(5)	157.6
C13−H13···S1 #4	0.93	2.71	3.483(4)	140.6
C5−H5···N1 #5	0.93	2.82	3.669(7)	151.7
C11−H11···N2 #6	0.93	2.59	3.669(7)	163.6
C12−H12···O4 #1	0.93	2.26	3.122(5)	153.0
C15−H15A···O3	0.97	2.32	3.256(6)	161.4
C19−H19B··· O5	0.97	2.43	3.317(14)	151.6
C19−H19B··· O6	0.97	2.72	3.498(16)	137.6
C19−H19A··· O3	0.97	2.29	3.230(16)	163.8
C19−H19A··· O4	0.97	2.70	3.279(15)	118.7
C20−H20A··· O1	0.97	2.49	3.341(14)	146.5
C20−H20A··· O2	0.97	2.56	3.342(15)	137.4
C20−H20B··· O7	0.97	2.36	3.294(17)	160.4
C20−H20B··· O8	0.97	2.51	3.133(16)	122.3

[a]Symmetry transformations used to generate equivalent atoms: #1 $-x + 1/2, -y + 1/2, -z + 1$ #2 $-x + 1, y, -z + 1/2$. #3 $-x + 1/2, y + 1/2, -z + 1/2$. #4 $x - 1/2, -y + 1/2, z + 1/2$. #5 $-x + 1/2, y - 1/2, -z + 1/2$. #6 $x, -y, z + 1/2$.

Crystal Structure Description of Compound 5. Compound **5** crystallizes in the triclinic system (from acetonitrile solvent) with space group $P\bar{1}$. A thermal ellipsoid plot of the asymmetric unit of the crystal structure of compound $[pseudorotoxane][Zn(dmit)_2]$ (**5**) is described in Figure 8a, which illustrates two halves of the psuedorotaxane molecules and one complex anion. The overall molecular structure is outlined in Figure 8b showing the DB24C8 wheel about the molecular dipyridinium axle (threading). In compound **5**, the $[Zn(dmit)_2]^{2-}$ anion exists in nonplanar geometry as presented in Figure 8c. Selected bond distances and angles in the crystal structure of compound **5** are described in Table S5 (Supporting Information). In the crystal structure, one $[Zn(dmit)_2]^{2-}$ anion brings four $[pseudorotaxane]^{2+}$ cations together, and likewise each rotaxane cation brings four $[Zn(dmit)_2]^{2-}$ anions together through the influence of C−H···S hydrogen bonding interactions as revealed in Figure S11 in the section of Supporting Information. As a result, a rectangular shape void space has been found to be generated by the assemblage of six pseudorotaxane cations, that are brought together by two

dx.doi.org/10.1021/cg500039y | Cryst. Growth Des. 2014, 14, 2343−2356

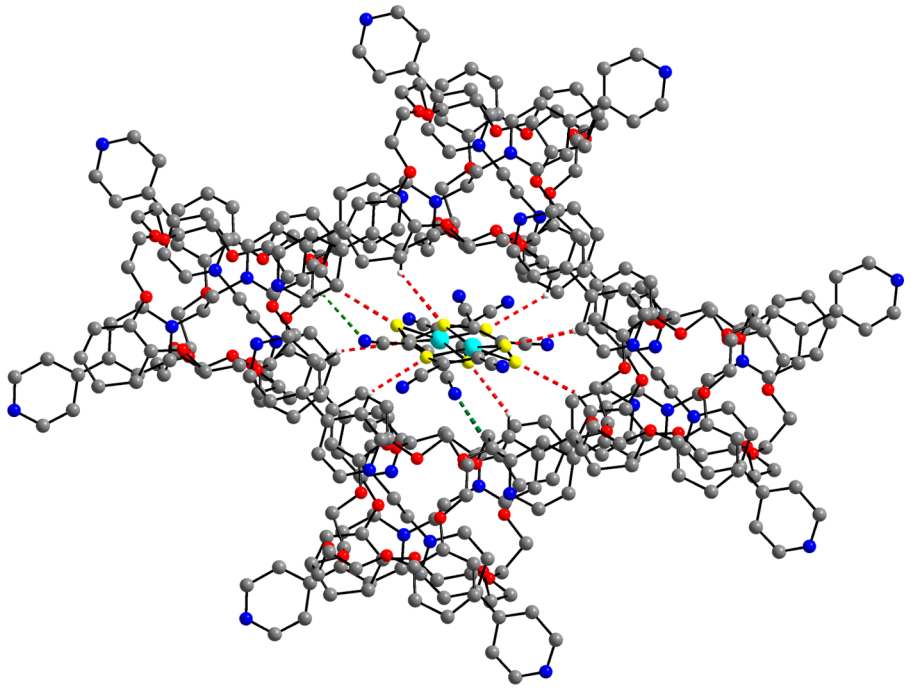

Figure 3. View of the formation of a void space, formed by the aggregation of pseudorotaxane cations, influenced by $[Cu(mnt)_2]^{2-}$ complex anions that are accommodated in the void space. The red dotted lines indicate C−H···S hydrogen bonding interactions, and the green dotted lines indicate C−H···N hydrogen bonding interactions between pseudorotaxane cations and $[Cu(mnt)_2]^{2-}$ complex anions. Color code: C, gray; N, blue; O, red; S, yellow; Cu, cyan.

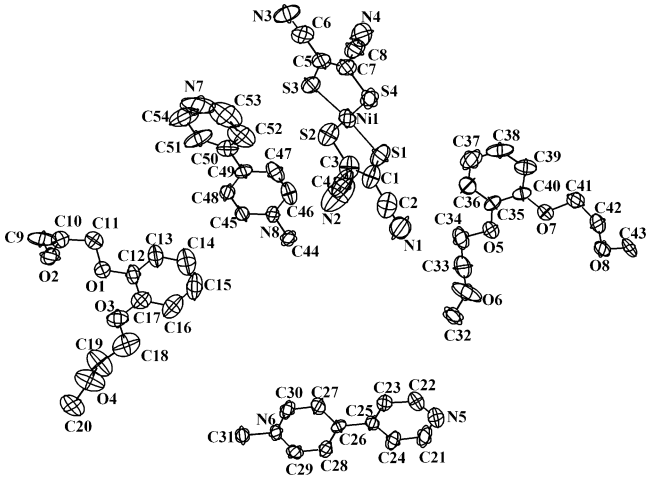

Figure 4. Thermal ellipsoid plot at the 50% probability level of the compound [pseudorotaxane] $[Ni(mnt)_2]$ (**2**).

$[Zn(dmit)_2]^{2-}$ anions through C−H···S and C−H···O hydrogen bonds (Table 7) including $\pi-\pi$ interactions, as depicted in Figure 9. Repetition of these rectangular voids in the relevant crystal brings about an arrangement as if the supramolecular ladders are laterally linked (Figure S13a, Supporting Information).

Alternatively, it can be described that, in the crystal of compound **5**, the pseudorotaxane units are arranged in a one-dimensional chainlike arrangement by $\pi-\pi$ stacking interactions that involve electron-poor aromatic rings of the bipyridinium axle giving rise to a linear horizontal supramolecular polypseudorotaxane strand. Interestingly, these horizontal strands are connected by vertical pseudorotaxane unit giving rise to the ladder kind of structure with the formation of infinite channels (Figure S13, Supporting Information). The vertical pseudorotaxane units are lined with strands by the assistance of $[Zn(dmit)_2]^{2-}$ complex anions that use C−H···S hydrogen bonding interactions. Two $[Zn(dmit)_2]^{2-}$ complex anions are embedded in each channel of ladders as shown in Figure S13b (Supporting Information). Thus, the existence of a ladder-like supramolecular architecture from cationic pseudorotaxane is strongly dependent on the anion, which in the present case is an inorganic coordination complex anion. Such a unique structural motif consisting of stacks of infinite supramolecular pseudorotaxane ladders, constructed by $\pi-\pi$ supramolecular interactions, mediated by $[Zn(dmit)_2]^{2-}$ complex anion, is a rare and attractive one. The closest Zn···Zn contact between two adjacent $[Zn(dmit)_2]^{2-}$ inorganic complex anions is 9.855(4) Å, which lie in the same void space of the ladder.

An Attempt to Remove the $[M(dithiolene)_2]^{2-}$ Complex Anion from the Ion Pair Compound [Pseudorotaxane][$M(mnt)_2$]/[Pseudorotaxane][$Zn(dmit)_2$] in a Solid−Liquid Interface Reaction without Dissolution of the Relevant Crystal. The present system deals with a series of ion pair compounds [pseudorotaxane]-$[M(mnt)_2]$ (M = Ni(II), Pd(II), Pt(II), Cu(II)) and [pseudorotaxane]$[Zn(dmit)_2]$, consisting of pseudorotaxane cations and metal dithiolato coordination complex anions $[M(mnt)_2]^{2-}$/$[Zn(dmit)_2]^{2-}$. In the crystal structures of compounds **1**, **2**, **3**, and **5**, the pseudorotaxane cations assemble into supramolecular architectures of diverse topologies having well-defined void spaces, and complex anions $[M(mnt)_2]^{2-}$/$[Zn(dmit)_2]^{2-}$ are located in these void spaces. To investigate whether the inorganic complex anion $[M(dithiolene)_2]^{2-}$ is ion exchangeable with other small anions in a solid−solution interface reaction, we suspended the deep brown crystals of [pseudorotaxane]$[Cu(mnt)_2]$ (**1**) in MeCN (in which the title

dx.doi.org/10.1021/cg500039y | *Cryst. Growth Des.* 2014, 14, 2343−2356

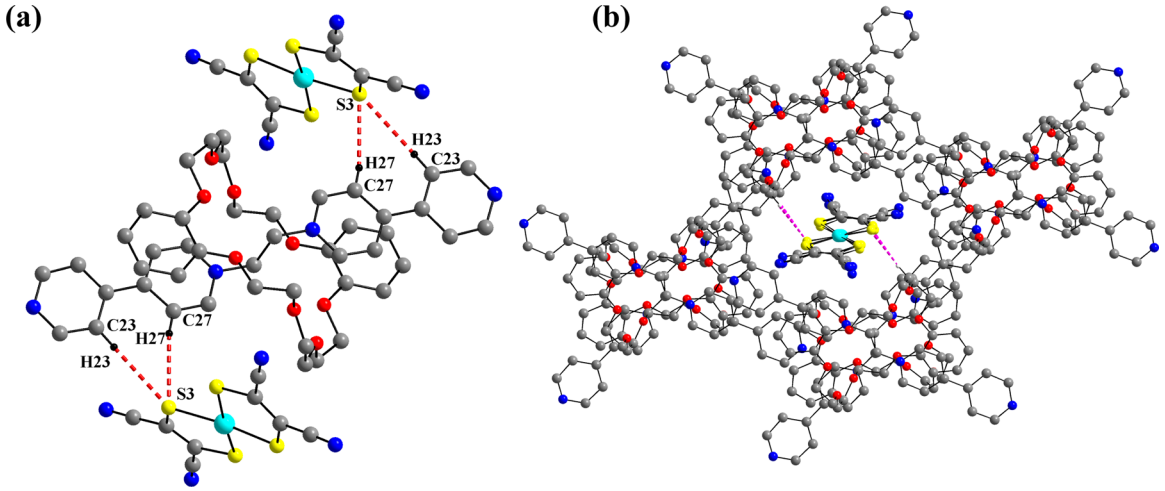

Figure 5. (a) The C−H···S hydrogen bonding interactions between an $[pseudorotaxane]^{2+}$ cation and two $[Ni(mnt)_2]^{2-}$ anions in the crystal structure of **2**; (b) the view of the formation of the void space, formed from the aggregation of cationic pseudorotaxanes, influenced by the coordination complex anion $[Ni(mnt)_2]^{2-}$, which is accommodated in the void space. The dotted lines indicate C−H···S hydrogen bonding interactions between pseudorotaxane cations and $[M(mnt)_2]^{2-}$ complex anions. Color code: C, gray; N, blue; O, red; S, yellow; Ni, cyan.

Table 4. Hydrogen Bonds for Compound 2[a]

D−H···A	d(D···H)	d(H···A)	d(D···A)	∠(DHA)
C27−H27···S3 #1	0.93	2.75	3.660(5)	165.9
C51−H51···N1 #2	0.93	2.75	3.440(11)	159.0
C19−H19···N3 #3	0.93	2.74	3.514(8)	141.3
C24−H24···N3 #4	0.93	2.70	3.615(7)	168.8
C28−H28···N3 #4	0.93	2.75	3.680(7)	175.7
C21−H21···N4 #5	0.93	2.56	3.446(8)	159.2
C33−H33A···N2 #6	0.97	2.74	3.629(10)	152.0
C31−H31A···O1 #7	0.97	2.62	3.430(5)	141.7
C31−H31A···O2 #7	0.97	2.54	3.289(6)	134.4
C31−H31B···O3 #7	0.97	2.96	3.566(6)	121.8
C31−H31B···O4 #7	0.97	2.62	3.564(6)	163.6
C44−H45B···O8 #8	0.97	2.92	3.494(5)	119.1
C44−H44A···O5 #8	0.97	2.40	3.362(7)	172.3
C44−H44A···O6 #8	0.97	2.61	3.436(5)	142.6
C44−H45B···O7 #8	0.97	2.56	3.266(6)	129.8

[a]Symmetry transformations used to generate equivalent atoms: #1 $-x + 1, -y + 1, -z + 1$; #2 $x - 1, y, z$; #3 $-x, -y + 1, -z + 1$; #4 $x, y - 1, z - 1$; #5 $-x + 1, -y, -z + 1$; #6 $x, y - 1, z$; #7 $-x, -y + 1, -z$; #8 $-x + 1, -y, -z + 1$.

Table 5. Hydrogen Bonds for Compound 3[a]

D−H···A	d(D···H)	d(H···A)	d(D···A)	∠(DHA)
C31−H31B···O8 #5	0.97	2.54	3.268(6)	131.4
C31−H31B···O7 #5	0.97	2.61	3.433(5)	142.6
C31−H31A···O5 #6	0.97	2.89	3.483(5)	120.4
C53−H53···O2 #5	0.93	2.61	3.409(6)	145.0
C54−H54B···O4 #5	0.97	2.64	3.572(6)	161.7
C54−H54B···O3 #5	0.97	2.94	3.555(6)	122.4
C54−H54A···O2 #5	0.97	2.53	3.297(6)	136.4
C54−H54A···O1 #5	0.97	2.62	3.434(5)	141.3
C44−H44···N4 #4	0.93	2.57	3.455(7)	159.6
C50−H50···N3 #3	0.93	2.75	3.675(6)	175.3
C47−H47···N3 #3	0.93	2.71	3.620(7)	167.8
C28−H28···N1 #2	0.93	2.94	3.790(8)	152.8
C23−H23···N1 #2	0.93	2.53	3.415(11)	160.0
C51−H51···S3 #1	0.93	2.73	3.643(4)	166.9
C46−H46···S3 #1	0.93	2.86	3.779(5)	172.1

[a]Symmetry transformations used to generate equivalent atoms: #1 $-x + 1, -y + 1, -z + 1$; #6 $x - 1, y, z$; #7 $x, y - 1, z - 1$; #8 $-x + 1, -y, -z + 1$; #9 $-x, -y + 1, -z$; #10 $-x + 1, -y, -z + 1$.

compounds are not soluble), and subsequently it was treated with saturated MeCN solution of $[Bu_4N]Br$. The deep brown crystals became off-white within an hour without their dissolution (Figure S14, Supporting Information). The off-white compound was separated out, and the resulting brown MeCN solution (filtrate) was slowly evaporated at room temperature affording microcrystalline solid of $[Bu_4N]_2[Cu(mnt)_2]$. Even though the resulting off-white crystals, that are obtained by anion exchange of single crystals of **1** with Br^- ($[Bu_4N]Br$ used as the Br^- source) in solid−liquid interface reaction, do not lose their overall crystallinity (as evidenced by their experimental PXRD pattern, Supporting Information), they lose their single crystallinity (as checked by single crystal X-ray diffraction). The IR spectrum of the off-white crystal (obtained by anion exchange, Figure S14, Supporting Information) does not show any characteristic bands for $[Cu(mnt)_2]^{2-}$ component, as evidenced by the absence of cyanide (CN) band in the region of 2200−2400 cm^{-1} and C═C band in the region of 1400−1480 cm^{-1} (for relevant IR spectra; see Figures S15 and S16 in the section of Supporting Information). This fact is consistent with the isolation of microcrystalline solid of $[Bu_4N]_2[Cu(mnt)_2]$ that was obtained by the evaporation of the ion-exchanged brown MeCN solution (filtrate, as discussed above). The X-ray powder pattern (Figure S17, Supporting Information) of the off-white compound ($[pseudorotaxane]Br_2$) does not match with the simulated X-ray powder pattern, obtained from single crystal data of compound $[pseudorotaxane][Cu(mnt)_2]$ (**1**). This means that supramolecular architecture of pseudorotaxane having well-defined void-spaces, observed in the crystal structure of compound **1**, is not retained in the crystal of $[pseudorotaxane]Br_2$, obtained from anion exchange experiment (after the exclusion of coordination complex anion $[Cu(mnt)_2]^{2-}$ from the relevant crystal). This experiment suggests that the supramolecular architectures having void spaces of different sizes and shapes, observed in the crystal structures of compounds **1**, **2**, **3**, and **5**, are formed by the supramolecular

dx.doi.org/10.1021/cg500039y | Cryst. Growth Des. 2014, 14, 2343−2356

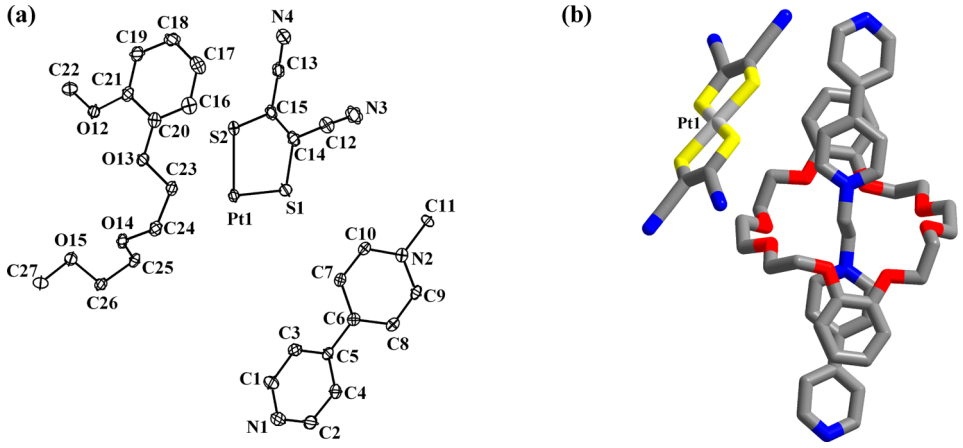

Figure 6. (a) Thermal ellipsoid plot at the 50% probability level of the compound [pseudorotoxane][Pt(mnt)$_2$] (**4**) and (b) the molecular structure of **4**; hydrogen atoms are omitted for clarity. Color code: C, gray; N, blue; O, red; S, yellow; Pt, white.

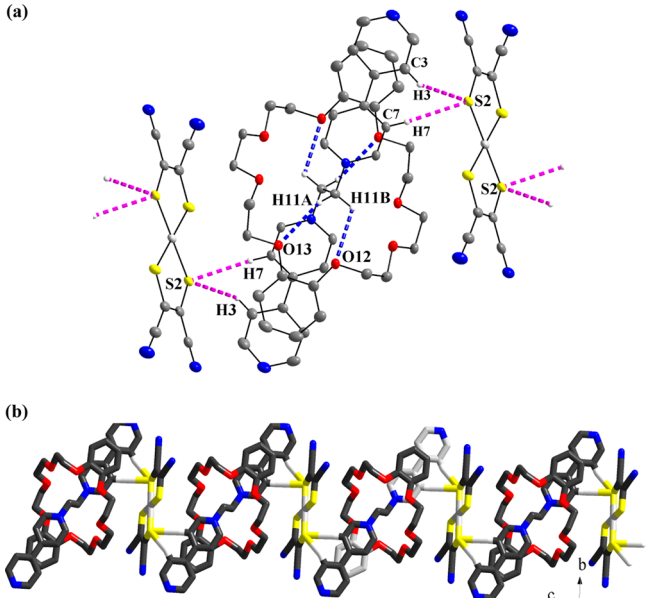

Figure 7. (a) The C–H···S hydrogen bonding interactions (magenta dotted lines) between an [pseudorotaxane]$^{2+}$ cation and two [Pt(mnt)$_2$]$^{2-}$ anions in the crystal structure of [pseudorotaxane][M(mnt)$_2$] (**4**), the blue dotted lines represent C–H···O hydrogen bonding interactions. (b) Wire-frame representation of chain-like arrangement consisting of alternating [pseudorotaxane]$^{2+}$ (cation) and [Pt(mnt)$_2$]$^{2-}$ (anion), formed by C–H···S hydrogen bonds in the crystal structure of [pseudorotaxane][M(mnt)$_2$] (**4**). Color code: C, gray; N, blue; O, red; S, yellow; Pt, white.

influence of the [M(mnt)$_2$]$^{2-}$/[Zn(dmit)$_2$]$^{2-}$ coordination complex anion, as if this complex anion brings the pseudorotaxane cations around it via weak interactions. The situation corresponds to the generation of void spaces, where this complex anion is located. Expectedly, once this complex anion is removed from the relevant crystal in a solid–liquid interface reaction, the supramolecular architecture of pseudorotaxane is not retained as observed in the crystal structures of compounds **1**, **2**, **3**, and **5**. The detailed structural information of the off-white compound ([pseudorotaxane]Br$_2$) is not yet known. The preparation of single crystal of this is under progress in our laboratory. The identity of [Cu(mnt)$_2$]$^{2-}$ component has been established by comparing the observed PXRD pattern of microcrystalline [Bu$_4$N]$_2$[Cu(mnt)$_2$], obtained by ion exchange of [pseudorotaxane][Cu(mnt)$_2$] (**1**) with Bu$_4$NBr in a solid–liquid interface reaction, with the simulated PXRD pattern, obtained from the single crystal data of [Bu$_4$N]$_2$[Cu(mnt)$_2$].[30] See Figure S18 (Supporting Information) for the observed and simulated PXRD patterns.

Table 6. Hydrogen Bonds in the Crystal Structure of Compound 4[a]

D–H···A	*d*(D···H)	*d*(H···A)	*d*(D···A)	∠(DHA)
C7–H7···S2 #1	0.93	2.81	3.732(3)	172.2
C3–H3···S2 #1	0.93	2.84	3.560(3)	135.1
C25–H25A···N3 #2	0.97	2.84	3.766(4)	160.0
C1–H1···N3 #2	0.93	2.76	3.612(5)	152.6
C17–H17···N4	0.93	2.92	3.819(4)	163.1
C19–H19···N4 #3	0.93	2.85	3.442(4)	122.4
C2–H2···N3 #4	0.93	2.60	3.366(4)	139.9
C4–H4···N4 #5	0.93	2.69	3.395(4)	133.5
C11–H11B···O15 #6	0.97	2.40	3.366(4)	172.8

[a]Symmetry transformations used to generate equivalent atoms: #1 $-x+2, -y+1, -z+1$; #2 $-x+1, -y+1, -z+1$; #3 $x, -y+3/2, z-1/2$; #4 $-x+1, y-1/2, -z+3/2$; #5 $-x+2, y-1/2, -z+3/2$; #6 $-x+2, -y+1, -z+1$.

How a [M(dithiolene)$_2$]$^{2-}$ Complex Anion Controls the Topology of the Void Space/Channel in the Supramolecular Architecture of Cationic Pseudorotaxane: Role of the Coordination Complex Anion. In three cases (compounds **1**, **2**, and **3** with M = Cu^{2+}, Ni^{2+}, and Pd^{2+} respectively), the single crystal X-ray structural determinations reveal that the respective complex anions get encapsulated in the void spaces of the pseudorotaxane architectures that are formed by the combination of hydrogen bonding and π–π stacking interactions. The bipyridinium axles of pseudorotaxanes interconnect among themselves by π–π stacking interactions in a criss-cross pattern leading to the formation of grid type of network structure. In the case of compound [pseudorotaxane][Cu(mnt)$_2$] (**1**), the complex anion [Cu(mnt)$_2$]$^{2-}$ has nonplanar geometry (see relevant crystal structure discussion, vide supra), and thus the outline/shape of the void space is rhombus-/diamond-like (see Figure S5 in the section of Supporting Information). On the other hand, for compounds [pseudorotaxane][Ni(mnt)$_2$] (**2**) and [pseudorotaxane][Pd(mnt)$_2$] (**3**), the complex anions [M(mnt)$_2$]$^{2-}$ (M = Ni^{2+} and Pd^{2+} respectively) exist, expectedly, in a planar geometry (see relevant crystal structure discussions,

dx.doi.org/10.1021/cg500039y | Cryst. Growth Des. 2014, 14, 2343–2356

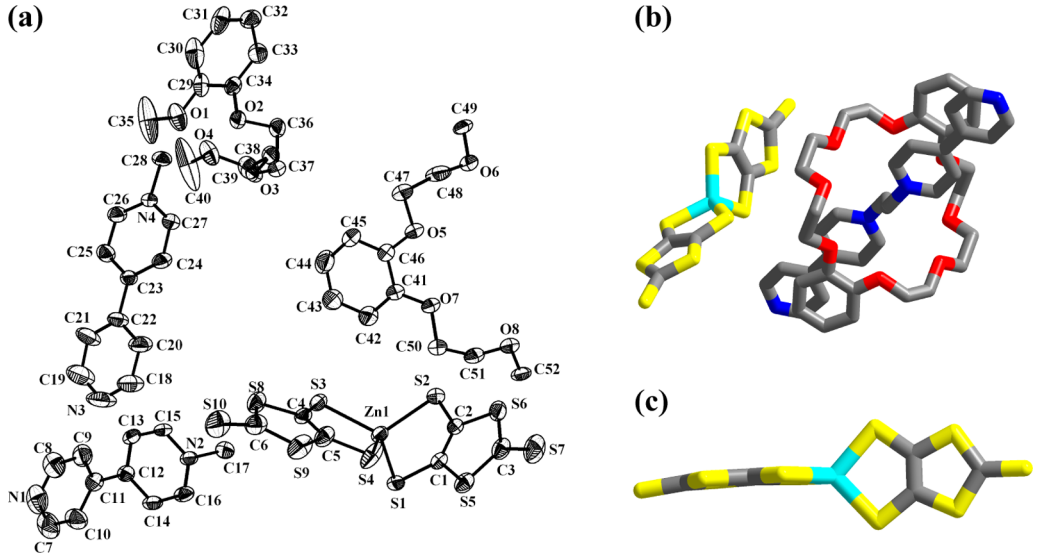

Figure 8. (a) Thermal ellipsoid plot at the 50% probability level of the compound [pseudorotoxane][Zn(dmit)$_2$] (**5**). (b) The molecular structure of **5**; hydrogen atoms are omitted for clarity. (c) The existence of $[Zn(dmit)_2]^{2-}$ complex anion showing its nonplanar geometry in compound **5**. Color code: C, gray; N, blue; O, red; S, yellow; Zn, cyan.

Table 7. Hydrogen Bonds in the Crystal Structure of Compound 5[a]

D−H···A	*d*(D···H)	*d*(H···A)	*d*(D···A)	∠(DHA)
C17−H17A···O7 #5	0.97	2.58	3.179(8)	120.0
C17−H17B···O5 #5	0.97	2.41	3.270(8)	148.1
C17−H17B···O6 #5	0.97	2.64	3.365(8)	131.8
C28−H28A···O4 #4	0.97	2.69	3.475(9)	138.9
C28−H28A···O1	0.97	2.31	3.145(9)	143.8
C28−H28B···O2	0.97	2.40	3.107(8)	129.3
C28−H28B···O3	0.97	2.42	3.326(8)	155.8
C50−H50B···S2	0.97	2.85	3.798(8)	166.1
C52−H52B···S2	0.97	2.96	3.917(7)	168.7
C30−H30···S6 #3	0.93	2.84	3.728(9)	159.5
C14−H14···S2 #2	0.93	2.77	3.601(6)	149.8
C13−H13···S1 #1	0.93	2.84	3.649(6)	146.7

[a]Symmetry transformations used to generate equivalent atoms: #1 $x-1, y-1, z$; #2 $x, y-1, z$; #3 $-x+1, -y+2, -z+2$; #4 $-x, -y+1, -z+2$; #5 $-x+1, -y+1, -z+1$.

vide supra), and both these cases, the square-like channels/void spaces (Figure S9, Supporting Information), are formed. In other words, the variation in shapes of the void spaces from rhombus-type (compound **1**) to square-type (compounds **2** and **3**) can also be correlated with the coordination geometry of the metal ion in the relevant coordination complex $[M(mnt)_2]^{2-}$ anions that are encapsulated in the respective void spaces ($[Cu(mnt)_2]^{2-}$ is quite nonplanar, whereas $[Ni(mnt)_2]^{2-}$ and $[Pd(mnt)_2]^{2-}$ are almost planar). In this series of compounds, the platinum analogue [pseudorotaxane][Pt(mnt)$_2$] (**4**), having same pseudorotaxane as cation (1,2-bis(4,4′-bipyridinium)ethane with dibenzo-24-crown-8), does not exhibit a supramolelcular framework having well-defined void spaces, as are observed in the crystal structures of compounds **1**, **2**, and **3**. We have attempted to explain this inconsistency by arguing that even the pseudorotaxane units would have constructed such a supramolecular array, found in the crystals of compounds **1**, **2** and **3**; the resulting void spaces could not have accommodated the relatively bigger anion $[Pt(mnt)_2]^{2-}$ (van der Waals radii: Pt 1.73 Å > Pd 1.63 Å ≥ Ni 1.63 Å > Cu 1.40 Å). Probably, for this reason, in the crystal structure of compound **4**, such grid-type void spaces, found in compounds **1**, **2**, and **3**, could not be formed; instead, it results in a packing arrangement (Figure S10, Supporting Information), as if it is the result of collapsing a grid-type of skeleton due to the insertion of the bigger sized guest $[Pt(mnt)_2]^{2-}$ in its void space.

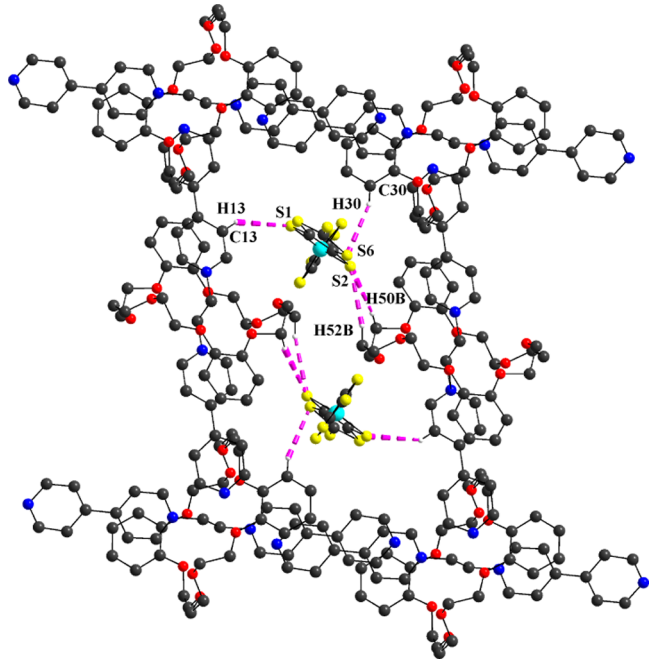

Figure 9. The view of the formation of the void space, formed from the aggregation of cationic pseudorotaxanes, influenced by the coordination complex anion $[Zn(dmit)_2]^{2-}$ anions, which is accommodated in the void space. The dotted lines indicate C−H···S hydrogen bonding interactions between pseudorotaxane cations and $[Zn(dmit)_2]^{2-}$ anions in compound [pseudorotoxane][Zn(dmit)$_2$] (**5**). Color code: C, gray; N, blue; O, red; S, yellow; Zn, cyan.

In the case of compound [pseudorotoxane][Zn(dmit)$_2$] (**5**), the cationic pseudorotoxane part is identical to that of

dx.doi.org/10.1021/cg500039y | *Cryst. Growth Des.* 2014, 14, 2343−2356

compounds **1**−**4**, but the anionic part is the bis(dithiolato)-zinc(II) complex anion, in which each dithiolate ligand has two rings (after its coordination to the metal ion) unlike the anionic part $[M(mnt)_2]^{2-}$ of compounds **1**−**4**, where only one ring is associated with each dithiolate ligand after its coordination to the metal ion. Thus, the topology of $[Zn(dmit)_2]^{2-}$ complex anion is different from that $[M(mnt)_2]^{2-}$ in terms of both size and shape. Even though compound **5** includes the same pseudorotoxane (as a cation) as included by compounds **1**−**4**, the grid-type of supramolecular architectures, formed in the crystals of compounds **1**−**3**, would not be expected to be formed in the case of compound **5** because of the relatively bigger size and different shape of $[Zn(dmit)_2]^{2-}$ complex anion. In the crystal structure of compound [pseudorotoxane][Zn-$(dmit)_2$] (**5**), we have seen a ladder-type of arrangement, and these ladders are laterally attached by supramolecular interactions in the relevant crystal (Figure S13, Supporting Information). The $[Zn(dmit)_2]^{2-}$ complex anions get encapsulated in each opening of the ladder. This complex anion is too large to be fitted into the grid type of void spaces, as were observed in the crystal structures of compounds **1**, **2**, and **3**. Thus, in this particular case, the $[Zn(dmit)_2]^{2-}$ complex anion has induced pseudorotaxane units to construct a ladder-type arrangement, in which the molecular plane of the encapsulated $[Zn(dmit)_2]^{2-}$ complex anion is perpendicular to the ladder plane (see Figure S12 in the section of Supporting Information).

We have seen, during analyzing suparamolecular features of compounds **1**−**5**, that the crystal structures of compounds **1**−**3** and **5** are characterized by well-defined void spaces, and the crystal structure of compound **4** does not exhibit such void spaces. To have more knowledge about the volumes of void spaces, we performed Platon solvent-accessible void calculations on the crystal structures of compounds **1**−**5**. As expected, the unit cell in the crystal structure of compound **4** contains no residual solvent-accessible voids. In the case of compound [pseudorotaxane][$Cu(mnt)_2$] (**1**), the total potential solvent area is 142.2 Å^3 per unit cell volume (2.6%), whereas the total potential solvent areas in the crystal structures of compounds [pseudorotaxane][$Ni(mnt)_2$] (**2**) and [pseudorotaxane][$Pd(mnt)_2$] (**3**) are 36.3 Å^3 per unit cell volume (1.3%) and 26.9 Å^3 per unit cell volume (1.0%) respectively (details of Platon potential solvent-accessible areas have been described as the last of part of Supporting Information). This variation (decreasing trend) in total potential solvent areas from 2.6% to 1.3% through 1.0% (from compound **1** to compound **2** through compound **3** respectively) can be explained by the ascending order of the molecular diameters (11.02 Å < 11.07 Å < 11.23 Å) of the complex anions $[Cu(mnt)_2]^{2-}$, $[Ni(mnt)_2]^{2-}$, and $[Pd-(mnt)_2]^{2-}$, that occupy the void spaces in their respective supramolecular host (pseudorotaxane) frameworks. It would be illogical to compare the total potential solvent area in the crystal structure of compound [pseudorotaxane][$Zn(dmit)_2$] (**5**) with potential solvent areas in the crystal structures of compounds **1**−**3**, because compound **5** is crystallized with a different type of dithiolato complex $[Zn(dmit)_2]^{2-}$ than $[M(mnt)_2]^{2-}$ type of dithiolate complex anion, present in compounds **1**−**3**.

Spectroscopy. The ^{1}H NMR spectra were recorded for compounds **2**−**5** in DMSO-d_6 solvent at 298 K. ^{1}H NMR chemical shifts of all compounds exhibit almost identical features, and the ^{1}H NMR data of the pseudorotoxane, used in the present study, are consistent with those of same pseudorotoxane from literature.[12b] A representative ^{1}H NMR spectrum of compound **2** is shown in Figure S17 (Supporting Information). The chemical shifts in the range of δ = 9.22−8.03 ppm correspond to the pyridine protons of 1,2-bis(4,4′-bipyridinium)ethane axle. The crown-ether phenyl ring protons appear in the range of 6.93−6.85 ppm. Chemical shifts in the range of δ = 5.31−3.34 ppm correspond to $-CH_2N^+$, $-CH_2-O-CH_2-$ protons. Because of the poor solubility of compounds **2**−**5**, we could not record their ^{13}C NMR spectra. The IR spectra of compound **1**−**4** exhibit the characteristic features for C≡N bonds of $[M(mnt)_2]^{2-}$ (M = Cu^{2+}, Ni^{2+}, Pd^{2+}, and Pt^{2+}) anions that appear in the range of 2189−2195 cm^{-1}. Compound [pseudorotoxane][$Zn(dmit)_2$] (**5**) shows IR bands at 1056 and 1022 cm^{-1}, which can be attributed to the C═S frequency of $dmit^{2-}$ ligand. Thus, the combination of ^{1}H NMR and IR spectral data strongly supports the association of $[M(dithiolene)_2]^{2-}$ anions with pseudorotaxane cation in title compounds.

The metal bis-dithiolene compounds are often highly colored due to the presence of delocalized π−electrons in these systems. The UV/vis−NIR spectra of compounds **1**−**5** were measured both in solution and the solid states at room temperature. The relevant spectral data with respective electronic transitions of compounds **1**−**5** are described in Table 8. The relevant absorption spectra of **1**−**5** are depicted in Figure S18 (Supporting Information). The deep-colored solutions of these classical inorganic complex anions $[M-(mnt)_2]^{2-}$ (M = Cu(II), Ni(II), Pd(II), and Pt(II)) exhibit the absorption bands in the region of 450−550 nm, which are generally assigned to a d(M)−π^*(mnt) metal−ligand charge transfer (MLCT) transition.[31] The lower wavelength bands in the region of 228−400 nm can be assigned to intraligand (mnt^{2-}: localized π−π^*) charge transfer transitions and the occurrence of ligand−metal charge transfer (LMCT) transitions. The longer wavelength absorption bands in the region of 650−1250 nm (for example, 870 nm for compound **2** and

Table 8. Absorption Spectral Data for Compounds 1−5 in DMF Solvent at 298 K

compound	wavelength[a] (ε)[b]	assignment
[pseudorotaxane][$Cu(mnt)_2$] (**1**)	321 (30000)	π−π^*
	354 (17000)	π−π^*
	426 (8500)	LMCT
	481 (7300)	MLCT
	1206 (85)	d−d
[pseudorotaxane][$Ni(mnt)_2$] (**2**)	274 (290000)	LMCT
	314 (156000)	π−π^*
	386 (36000)	LMCT
	480 (21000)	MLCT
	871 (200)	d−d
[pseudorotaxane][$Pd(mnt)_2$] (**3**)	270 (180000)	LMCT
	448 (17000)	MLCT
	691 (60)	d−d
[pseudorotaxane][$Pt(mnt)_2$] (**4**)	266 (88000)	LMCT
	339 (24000)	π−π^*
	482 (7000)	MLCT
	626 (710)	d−d
[pseudorotaxane][$Zn(dmit)_2$] (**5**)	312 (5000)	π−π^*
	512 (33000)	n−π^*

[a]In nm. [b]In M^{-1} cm^{-1}.

dx.doi.org/10.1021/cg500039y | Cryst. Growth Des. 2014, 14, 2343−2356

Scheme 6

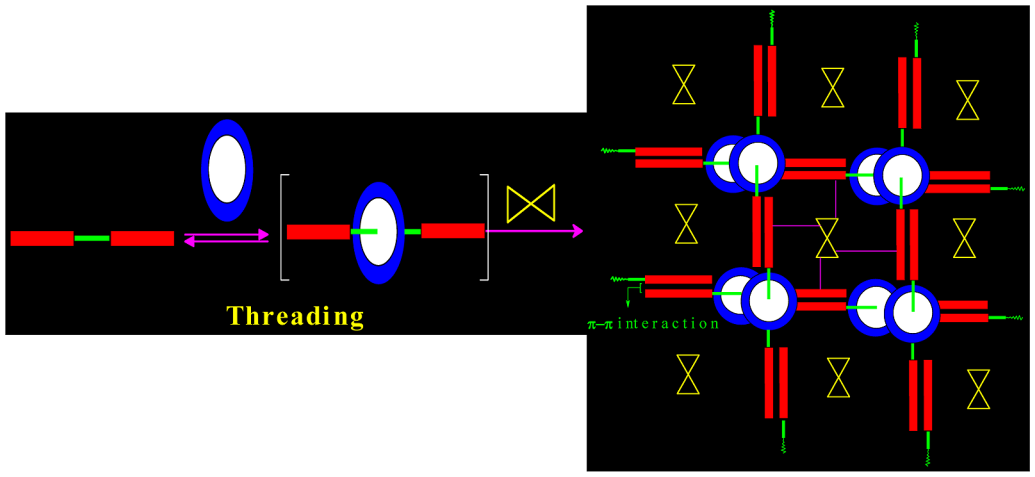

1210 nm for compound **1**) appear due the existence of *d*–*d* transitions.[32]

The ESR spectrum of compound **1** was measured in DMF both at liquid nitrogen and room temperature (relevant ESR plots are shown in Figure S19 in the section of Supporting Information). At liquid nitrogen temperature, it exhibits hyperfine structure due to the presence of ^{63,65}Cu nuclei. Interestingly, both $g_{\|}$ and $g_{\perp}$ features are resolved due to ^{63,65}Cu hyperfine coupling, which is very rarely observed in metal–dithiolene complexes.[33] The average value of the hyperfine coupling parameters (determined from $|A_{\|}|$ = 15.3 mT and $|A_{\|}|$ = 4.8 mT) is 8.3 mT, which is not identical to that (7.4 mT) of the solution ESR spectrum at room temperature.

SUMMARY: CONCLUSIONS

Metal bis(dithiolato) complexes have been reported in numerous contexts, namely, NIR materials, conductive molecules, potential catalysts, magnetic materials, ion pair charge transfer complexes, nonlinear optical materials, bio-inorganic model systems to mimic the active sites of metallo-enzymes, etc. Similarly, rotaxane-/pseudorotaxane-systems have been described in versatile perspectives, for example, molecular actuators and switches within mesoscale molecular electronics devices. Thus, these two different systems have importance in their own perceptions. Keeping in mind the fact that the supramolecular assembly of cationic pseudorotaxane-systems with anionic metal bis(dithiolato) complexes are considered to be significant through the electrostatic aggregation, we intended to investigate the results of interaction of these two systems (cationic pseudorotaxane and anionic metal bis(dithiolato) complexes) on the basis of electrostatic molecular assembly as well as to see the role of metal bis(dithiolato) complexes and pseudorotaxanes on the supramolecular assembly. Thus, a series of ion-pair compounds $\{[PR]^{2+}[ML_2]^{2-}\}$ has been synthesized by the combination of classical metal bis-dithiolene inorganic complex anions $[M(dithiolato)_2]^{2-}$ (M = Cu(II) (**1**), Ni(II) (**2**), Pd(II) (**3**), Pt(II) (**4**) and Zn(II) (**5**); dithiolene = mnt^{2-} and $dmit^{2-}$) with cationic $[pseudorotaxane]^{2+}$. We have demonstrated that the cationic supramolecular pseudorotaxane architectures are influenced by the coordination complex anions through electrostatic interactions leading to noncovalent architectures of diverse topologies. The formation of such supramolecular architectures, controlled by a combination of electrostatic interaction and hydrogen bonding interactions between the cation and anions, is schematically presented in Scheme 6.

Since the syntheses of title compounds are performed in situ, that is, it includes the addition of axle (bipyridinium derivative), wheel (crown ether), and the coordination complex in one pot, the construction of such supramolecular architectures can be speculated as the threading of the wheel followed by their aggregation under the influence of the coordination complex anion (Scheme 6). This work has opened a new research opportunity in the area of inorganic supramolecular chemistry that may include electrostatic interactions/aggregations between anionic $[M(dithiolato)_2]^{2-}$ coordination complex anions and varieties of mechanically interlocked cationic systems, such as cyclophanes, rotaxanes, and catenanes.

ASSOCIATED CONTENT

Supporting Information

Supplementary figures related to crystal structures for title compounds, PXRD patterns, IR, ^{1}H NMR, EPR and UV–visible spectra, supplementary tables related to crystal structures. This information is available free of charge via the Internet at http://pubs.acs.org/.

AUTHOR INFORMATION

Corresponding Author

*E-mail: skdsc@uohyd.ernet.in; samar439@gmail.com; fax: +91-40-2301-2460; tel: +91-40-2301-1007.

Notes

The authors declare no competing financial interest.

ACKNOWLEDGMENTS

The authors thank CSIR, Government of India (Project No. 01 (2556)/12/EMR-II) for financial support. The National X-ray Diffractometer facility at University of Hyderabad by the Department of Science and Technology, Government of India, is gratefully acknowledged. Our special thanks are due to Dr. Bharat Kumar Tripuramallu for his help in analyzing crystal structures.

REFERENCES

(1) (a) Livoreil, A.; Dietrich-Buchecker, C. O.; Sauvage, J.-P. *J. Am. Chem. Soc.* **1994**, *116*, 9399. (b) Raehm, L.; Kern, J.-M.; Sauvage, J.-P. *Chem. Eur. J.* **1999**, *5*, 3310. (c) Amabilino, D. B.; Stoddart, J. F. *Chem. Rev.* **1995**, *95*, 2725. (d) Dietrich-Buchecker, C. O.; Sauvage, J.-P.;

Kintzinger, J. P. *Tetrahedron Lett.* **1983**, *24*, 5095. (e) Sauvage, J.-P. *Acc. Chem. Res.* **1990**, *23*, 319. (f) Dietrich-Buchecker, C.; Sauvage, J.-P. *Chem. Rev.* **1987**, *87*, 795.
(2) (a) Schill, G. *Catenanes, Rotaxanes and Knots*; Academic Press: New York, 1971. (b) Sauvage, J.-P., Dietrich-Buchecker, C., Eds. *Molecular Catenanes, Rotaxanes, and Knots*; Wiley-VCH: Weinheim, 1999.
(3) (a) Hunter, C. A. *J. Am. Chem. Soc.* **1992**, *114*, 5303. (b) Vögtle, F.; Meier, S.; Hoss, R. *Angew. Chem., Int. Ed.* **1992**, *31*, 1619. (c) Jonston, A. G.; Leigh, D. A.; Pritchard, R. J.; Deegan, M. D. *Angew. Chem., Int. Ed.* **1995**, *34*, 1209. (d) Sambrook, M. R.; Beer, P. D.; Wisner, J. A.; Paul, R. L.; Cowley, A. R.; Szemes, F.; Drew, M. G. B. *J. Am. Chem. Soc.* **2005**, *127*, 2292. (e) Wang, X.-L.; Qin, C.; Wang, E.-B. *Cryst. Growth Des.* **2006**, *6*, 439.
(4) (a) Hogg, L.; Leigh, D. A.; Lusby, P. J.; Morelli, A.; Parsons, S.; Wong, J. K. Y. *Angew. Chem., Int. Ed.* **2004**, *43*, 1218. (b) Hori, A.; Kumazawa, K.; Kusukawa, T.; Chand, D. K.; Fujita, M.; Sakamoto, S.; Yamaguchi, K. *Chem. Eur. J.* **2001**, *7*, 4142. (c) McArdle, C. P.; Irwin, M. J.; Jennings, M. C.; Puddephat, R. J. *Angew. Chem., Int. Ed.* **1999**, *38*, 3376. (d) Vance, A. L.; Alcock, N. W.; Heppert, J. A.; Busch, D. H. *Inorg. Chem.* **1998**, *37*, 6912. (e) Aucagne, V.; Hänni, K. D.; Leigh, D. A.; Lusby, P. J.; Walker, D. B. *J. Am. Chem. Soc.* **2006**, *128*, 2186. (f) Yu, L.; Li, M.; Zhou, X.-P.; Li, D. *Inorg. Chem.* **2013**, *52*, 10232. (g) Gao, C.-Y.; Zhao, L.; Wang, M. -X. *J. Am. Chem. Soc.* **2011**, *133*, 8448.
(5) (a) Raymo, F. M.; Stoddart, J. F. *Chem. Rev.* **1999**, *99*, 1643. (b) Flood, A. H.; Ramirez, R. J. A.; Deng, W.-Q.; Muller, R. P.; Goddard, W. A.; Stoddart, J. F. *Aust. J. Chem.* **2004**, *57*, 301. (c) Try, A. C.; Harding, M. M.; Hamilton, D. G.; Sanders, J. K. M. *Chem. Commun.* **1998**, 723. (d) Loeb, S. J.; Wisner, J. A. *Chem. Commun.* **2000**, 845. (e) Ashton, P. R.; Ballardini, R.; Balzani, V.; Bêlohradsky, M.; Gandolfi, M. T.; Philp, D.; Prodi, L.; Raymo, F. M.; Reddington, M. V.; Spencer, N.; Stoddart, J. F.; Venturi, M.; Williams, D. J. *J. Am. Chem. Soc.* **1996**, *118*, 4931. (f) Stoddart, J. F.; Tseng, H.-R. *Proc. Natl. Acad. Sci. U.S.A.* **2002**, *99*, 4797. (g) Raymo, F. M.; Houk, K. N.; Stoddart, J. F. *J. Am. Chem. Soc.* **1998**, *120*, 9318. (h) Ashton, P. R.; Baxter, I.; Fyfe, M. C. T.; Raymo, F. M.; Spencer, N.; Stoddart, J. F.; White, A. J. P.; Williams, D. J. *J. Am. Chem. Soc.* **1998**, *120*, 2297.
(6) (a) Kaiser, G.; Jarrosson, T.; Otto, S.; Ng, Y.-F.; Bond, A. D.; Sanders, J. K. M. *Angew. Chem., Int. Ed.* **2004**, *43*, 1959. (b) Kwan, P. H.; Swager, T. M. *J. Am. Chem. Soc.* **2005**, *127*, 5902.
(7) (a) Kim, K.; Kim, D.; Lee, J. W.; Ko, Y. H.; Kim, K. *Chem. Commun.* **2004**, 848.
(8) (a) Sauvage, J. -P. *Chem. Commun.* **2005**, 1507. (b) Weber, N.; Hamann, C.; Kern, J. −M.; Sauvage, J.-P. *Inorg. Chem.* **2003**, *42*, 6780. (c) Sauvage, J. -P. *Acc. Chem. Res.* **1998**, *31*, 611. (d) Chambron, J. −C.; Dietrich- Buchecker, C. O.; Nierengarten, J.-F.; Sauvage, J.-P. *Pure Appl. Chem.* **1994**, *66*, 1543. (e) Collin, J.-P.; Dietrich-Buchecker, C. O.; Gaviña, P.; Jimenez-Molero, M. C.; Sauvage, J.-P. *Acc. Chem. Res.* **2001**, *34*, 477. (f) Jimenez, M.-C.; Dietrich- Buchecker, C.; Sauvage, J.-P.; De Cian, A. *Angew. Chem., Int. Ed.* **2000**, *39*, 1295. (g) Létinois-Halbes, U.; Hanss, D.; Beierle, J. M.; Collin, J.-P.; Sauvage, J.-P. *Org. Lett.* **2005**, *7*, 5753.
(9) Loeb, S. J.; Wisner, J. A. *Angew. Chem., Int. Ed.* **1998**, *37*, 2838.
(10) Loeb, S. J.; Wisner, J. A. *Chem. Commun.* **1998**, 2757.
(11) Loeb, S. J.; Wisner, J. A. *Chem. Commun.* **2000**, 845.
(12) (a) Loeb, S. J.; Wisner, J. A. *Chem. Commun.* **2000**, 1939. (b) Loeb, S. J.; Tiburcio, J.; Vella, S. J.; Wisner, J. A. *Org. Biomol. Chem.* **2006**, *4*, 667.
(13) (a) Hubbard, L.; Davidson, G. J. E.; Patel, R. H.; Wisner, J. A.; Loeb, S. J. *Chem Commun.* **2004**, 138. (b) Davidson, G. J. E.; Loeb, S. J.; Parekh, N. A.; Wisner, J. A. *J. Chem. Soc., Dalton Trans.* **2001**, 3135−3136.
(14) (a) Hoffart, D. J.; Loeb, S. J. *Angew. Chem., Int. Ed.* **2005**, *44*, 901. (b) Davidson, G. J. E.; Loeb, S. J. *Angew. Chem., Int. Ed.* **2003**, *42*, 74. (c) Loeb, S. J. *Chem. Commun.* **2005**, 1511.
(15) Gibson, H. W.; Yamaguchi, N.; Jones, J. W. *J. Am. Chem. Soc.* **2003**, *125*, 3522.
(16) (a) Tiburcio, J.; Davidson, G. J. E.; Loeb, S. J. *Chem. Commun.* **2002**, 1282. (b) Hu, X.-Y.; Zhang, P.; Wu, X.; Xia, W.; Xiao, T.; Jiang, J.; Lin, C.; Wang, L. *Polymer Chemistry* **2012**, *3*, 3060. (c) Yan, X.; Wu, X.; Wei, P.; Zhang, M.; Haung, F. *Chem. Commun.* **2012**, *48*, 8201. (d) Loeb, S. J. *Chem. Soc. Rev.* **2007**, *36*, 226. (e) Nikitin, K.; Müller-Bunz, H. *New J. Chem.* **2009**, *33*, 2472. (f) Saha, S.; Ghosh, P. *J. Chem. Sci.* **2012**, *124*, 1229. (g) Valderrey, V.; Escudero-Adàn, E. C.; Ballester, P. *J. Am. Chem. Soc.* **2012**, *134*, 10733. (h) Moreno-Olivares, S. I.; Cervantes, R; Tiburcio, J. *J. Org. Chem.* **2013**, *78*, 10724. (i) Samsam, S.; Leclercq, L.; Schmitzer, A. R. *J. Phys. Chem. B* **2009**, *113*, 9493. (j) Li, J.-S.; Fan, M.-L.; Chen, L.-G.; Hökelek, T.; Haung, P.-M. *Mol. Cryst. Liq. Cryst.* **2010**, *517*, 3. (k) Castillo, D.; Astudillo, P.; Mares, J.; Gonzàlez, F. J.; Vela, A.; Tiburcio, J. *Org. Biomol. Chem.* **2007**, *5*, 2252. (l) Loeb, S. J.; Tiburcio, J.; Vella, S. J. *Org. Lett.* **2005**, *7*, 4923. (m) Han, Y.; Gu, Y.-K.; Xiang, J.-F.; Chen, C.-F. *Chem. Commun.* **2012**, *48*, 11076.
(17) (a) Mercuri, M. L.; Deplano, P.; Pilia, L.; Serpe, A.; Artizzu, F. *Coord. Chem. Rev.* **2010**, *254*, 1419. (b) Kean, C. L.; Pickup, P. G. *Chem. Commun.* **2001**, 815. (c) Wang, F.; Reynolds, J. R. *Macromolecules* **1990**, *23*, 3219. (d) Baudron, S. A.; Hosseini, M. W. *Inorg. Chem.* **2006**, *45*, 5260. (e) Weis, E. M.; Barnes, C. L.; Duval, P. B. *Inorg. Chem.* **2006**, *45*, 10126. (f) Ribas, X.; Maspoch, D.; Dias, J.; Morgado, J.; Almeida, M.; Wurst, K.; Vaughan, G.; Veciana, J.; Rovira, C. *CrystEngComm* **2004**, *6*, 589. (g) Ribas, X.; Dias, J.; Morgado, J.; Wurst, K.; Almeida, M.; Veciana, J.; Rovira, C. *CrystEngComm* **2002**, *4*, 564. (h) Kean, C. L.; Miller, D. O.; Pickup, P. G. *J. Mater. Chem.* **2002**, *12*, 2949.
(18) (a) Vogel, A. I. In *Text Book of Practical Organic Chemistry*, 4th ed.; English Language Book Society and Longman: London, 1978, p 264. (b) Perrin, D. D.; Armarego, W. L. F.; Perrin, D. R. In *Purification of laboratory Chemicals*; Pergamon Press: London, 1966.
(19) Davison, A.; Holm, R. H. *Inorg. Synth.* **1967**, *10*, 8.
(20) Svenstrup, N.; Becher, J. *Synthesis* **1995**, 215.
(21) *Software for the CCD Detector System*; Bruker Analytical X-Ray Systems Inc.: Madison, WI, 1998.
(22) Sheldrick, G. M. *SADABS, A Program for Absorption Correction with the Siemens SMART Area-Detector System*; University of Göttingen: Germany, 1996.
(23) Sheldrick, G. M. *SHELXS-97, A Program for Solution of Crystal Structures*; University of Göttingen: Germany, 1997.
(24) Sheldrick, G. M. *SHELXL-97, A Program for Refinement of Crystal Structures*; University of Göttingen: Germany, 1997.
(25) Madhu, V.; Das, S. K. *Polyhedron* **2004**, *23*, 1235.
(26) (a) Domagala, M.; Grabowski, S. J.; Urbaniak, K.; Mloston, G. *J. Phys. Chem. A* **2003**, *107*, 2730. (b) Domagala, M.; Grabowski, S. J. *J. Phys. Chem. A* **2005**, *109*, 5683. (c) Muthu, S.; Vittal, J. J. *Cryst. Growth Des.* **2004**, *4*, 1181.
(27) (a) Borrmann, H.; Persson, I.; Sandström, M.; Stälhandske, C. M. V. *J. Chem. Soc., Perkin Trans.* **2000**, *2*, 393. (b) Ohkita, M.; Suzuki, T.; Nakatani, K.; Tsuji, T. *Chem. Commun.* **2001**, 1454.
(28) Harris, S. *Polyhedron* **1989**, *8*, 2843.
(29) Tiburcio, J.; Davidson, G. J. E.; Loeb, S. J. *Chem. Commun.* **2002**, 1282.
(30) Plumlee, K. W.; Hoffman, B. M.; Ibers, J. A.; Soos, Z. G. *J. Chem. Phys.* **1975**, *63*, 1926.
(31) Shupack, S. I.; Billig, E.; Clark, R. J. H.; Williams, R.; Gray, H. B. *J. Am. Chem. Soc.* **1964**, *86*, 4594.
(32) Persaud, L.; Langford, C. H. *Inorg. Chem.* **1985**, *24*, 3562.
(33) (a) Matsubayashi, G.; Takahashi, K.; Tanaka, T. *J. Chem. Soc., Dalton Trans.* **1988**, 967. (b) Mahadevan, C.; Seshasayee, M. *J. Crystallogr. Spectrosc. Res.* **1984**, *14*, 215.